ANTIMONY MÖSSBAUER STUDIES

A MÖSSBAUER SPECTROSCOPIC INVESTIGATION

OF

INORGANIC ANTIMONY COMPOUNDS

By

BASIL P. DELLA VALLE, B.Sc.

A Thesis

Submitted to the Faculty of Graduate Studies

in Partial Fulfillment of the Requirements

for the Degree

Master of Science

McMaster University

May 1971

MASTER OF SCIENCE (1971)   McMASTER UNIVERSITY
(Chemistry)   Hamilton, Ontario

TITLE: A Mössbauer Spectroscopic Investigation of Inorganic
         Antimony Compounds

AUTHOR: Basil Patrick Della Valle, B.Sc.   (McMaster University)

SUPERVISOR: Dr. T. Birchall

NUMBER OF PAGES: vii, 71

ABSTRACT

In this thesis the Mössbauer spectroscopic technique was applied to a wide variety of antimony compounds.

Antimony chalcogenides, oxides and a phosphate were studied. No evidence could be found to support the existence of Sb_2S_5. Sb_2O_4 was found to contain Sb(III) and Sb(V) rather than Sb(IV). $SbPO_4$ and the Sb(III) site in Sb_2O_4 had similar Mössbauer parameters in agreement with their structures.

Hexahalo complexes of antimony, some of which contain both (III) and (V) oxidation states, have been examined. These exhibit extremely large isomer shifts which are interpreted as indicating no involvement of the 5s electron pair of Sb in the bonding scheme.

A study was made of some antimony-fluorine systems. The spectra of $KSbF_5$, $KSbF_4$ and KSb_2F_7 and similar salts were interpreted in terms of the known structures. Other complex antimony fluorides and fluorosulphates have also been examined and possible structures suggested.

Three antimony-containing minerals, nadorite, tetrahedrite, and boulangerite have been examined, and attempts made to rationalise the Mössbauer data in terms of known structural parameters.

ACKNOWLEDGEMENTS

TABLE OF CONTENTS

LIST OF TABLES

LIST OF FIGURES

CHAPTER I

Introduction

Shortly after the decay scheme for ^{121m}Sn was clarified[1,2], it was shown by Snyder and Beard[3] that the 37.2 Kev level in ^{121}Sb was suitable for Mössbauer effect studies. Ruby et al. in a series of papers[4-7] pioneered ^{121}Sb Mössbauer spectroscopy and its applications to chemical problems. Their first effort[4] was to measure the previously unknown quadrupole moment of the first excited state (+ 7/2), or more exactly the ratio $R_q = Q(7/2) / Q(5/2)$, by studying the quadrupole resonance in cubic Sb_2O_3. They found $R_q = 1.38 \pm 0.02$ and using $Q(5/2) = -(0.54 \pm 0.07)b$ from optical spectroscopy obtained a value for $Q(7/2) = -(0.75 \pm 0.09)b$. The quadrupole splitting was measured as $+18.8 \pm 0.8$ mm/sec. The sign, which implies a negative field gradient at the Sb nucleus, was interpreted as being consistent with partially covalent bonding of the 5p electrons to the three nearest oxygen atoms. Ruby et al.[5] then studied the Mössbauer resonance in ferromagnetic MnSb at 4.2°K and obtained a magnetic spectrum (18 transitions allowed) consisting of four prominent lines of about equal intensity and two pairs of weaker satellites on each side of this group. From this spectrum they obtained a value for the previously unknown ratio $R_m = g(7/2)/g(5/2)$ of 0.498 ± 0.005 and thus from the known ground state magnetic moment, $\mu(5/2) = 3.359$ nm, they obtained the moment for the excited state $\mu(7/2) = +2.35 \pm 0.03$ nm. Later, Ruby et al.[6] measured the isomer

1

shift and quadrupole splitting of a variety of antimony compounds
which were believed to be isoelectronic with analogous tin compounds
to allow comparison of their isomer shifts. In this way, $\Delta R/R$ for
^{121}Sb was found to be approximately 6.5 times larger than that for
^{119}Sn, but of opposite sign. A value of $(-8.5 \pm 3.0) \times 10^{-4}$ was
obtained.

In 1968, three papers by Russian workers appeared in the liter-
ature. V. A. Brukhanov et al.[8] measured the isomer shift in iso-
electronic six coordinate antimony salts such as $NaSbF_6$, $NaSb(OH)_6$,
and $HSbCl_6 \cdot xH_2O$. A linear dependence of the isomer shift on ligand
electronegativity was found similar to that for six coordinate tin
compounds of the type, $SnHal_6^{-2}$. V. Kotkhekar et al.[9] studied the
isomer shifts for the trivalent antimony halides ($SbCl_3$, $SbBr_3$, SbI_3)
and found the isomer shift increased linearly with increased ionicity
of the bonds. Gukasyan and Shpinel[10] measured the isomer shifts in
organo-antimony compounds of the type Ar_3SbX, Ar_4SbX, and Ar_3Sb. The
spectra recorded at 78°K were found to be broad single lines with
appreciable asymmetry.

A second major contribution to the chemical application of ^{121}Sb
Mössbauer spectroscopy has been made by G. G. Long and his coworkers.
An investigation of the sulphides of antimony[11] resulted in the
discovery that the so-called antimony pentasulphide had a variable
sulphur content and that the isomer shift for the "pentasulphide"
was located in the antimony (III) region of the velocity range. This
suggested that the antimony atom exists in the +3 oxidation state
rather than the +5 state. Long et al.[12] have reported on the

various oxides of antimony, namely cubic, orthorhombic and amorphous Sb_2O_3, α-Sb_2O_4 and Sb_2O_5. They found that all of the spectra, except α-Sb_2O_4, consisted of single, quadrupole split absorptions. However, the α-Sb_2O_4 showed two completely resolved peaks of equal area which had isomer shifts characteristic of Sb(III) and Sb(V). This indicated that α-Sb_2O_4 contains antimony in two oxidation states [Sb(III), Sb(V)] rather than Sb(IV). In a further paper, Long et al.[13] reported on the Mössbauer spectra of the simple antimony halides, as well as cubic Sb_2O_3. A linear relationship between isomer shift and ligand-metal electronegativity difference was found for Sb_2O_3, $SbCl_3$, $SbBr_3$ and SbI_3 and interpreted as being due to constant "s" character in the ligand-metal bonds. However, antimony trifluoride did not obey this relationship. It was assumed that this was because SbF_3 has a different structure to that of the other trihalides. More recently, Long et al.[14] have investigated a series of 21 organo-antimony compounds of the type Ph_3SbX_2, Ph_4SbX at 80°K and 12 of these at 4.2°K. The various Mössbauer parameters could be determined much more readily and precisely at 4.2°K due to the marked increase in the per cent effect. Of the compounds studied Ph_4SbClO_4 was the only compound found to contain a Ph_4Sb^+ cation in the solid state. The differences in the Mössbauer parameters for the various series studied were discussed in terms of likely bond hybridizations and structures of the compounds. As a direct result of this paper, Stevens and Ruby[15] made use of organic compounds such as $(C_6H_5)_3SbCl_2$ which have larger electric field gradients than Sb_2O_3 to improve the accuracy of $R = Q^*/Q$. The new value for R is 1.34 ± 0.01. Long and

Bowen[16] investigated the decomposition of Schlippe's salt $Na_3SbS_4 \cdot 9H_2O$. They found that there are at least two modes of decomposition of the salt. Dehydration results in the loss of water with little change in the antimony atom environment as evidenced by the unchanged Mössbauer spectra. When Schlippe's salt is exposed to air for long periods of time the decomposition products show two antimony (V) peaks, one of which is similar to that in Schlippe's salt and the other which has an isomer shift value consistent with compounds having Sb(V) bound to oxygen rather than sulphur. Dokuzoguz et al.[17] used Mössbauer spectroscopy to determine the isomer shifts of ^{121}Sb III-V semiconductors, InSb, GaSb, and AlSb. In this series it was found that the "s" electron density shifts slightly towards the Gp III atom in the order In < Ga < Al. This was interpreted as indicating a greater extent of electron transfer from the Gp V to Gp III atom occurring in AlSb than in GaSb, with InSb having the least transfer. Russian workers, Golovnin et al.[18], have examined the magnetic spectrum of ^{121}Sb in yttrium iron garnet. The experimentally observed spectrum closely resembled that of MnSb reported by Ruby.[5] An internal magnetic field of 290 ± 10 K_{oe} was found.

The feasibility of obtaining useful chemical information from ^{121}Sb Mössbauer was clearly shown by Ruby's[4-7] initial work and the present work which followed up these earlier investigations. Reported in this thesis are studies carried out on various groups of antimony compounds including the antimony chalcogenides, oxides and phosphate, chloro complexes of antimony, fluoro anions of antimony, complex fluorides and fluorosulphates, and a few antimony-containing minerals.

CHAPTER II

Theory

1. The Mössbauer Effect

Many radioactive nuclei in an excited state emit γ-rays and thereby reach the ground state of the nucleus with the same mass number and same charge. If these γ-rays are allowed to interact with a similar ground state nucleus the γ-rays may be reabsorbed in a resonance capture process. This process was at first thought to be an inefficient one because, although most of the nuclear transition energy appeared as γ-ray energy, a small, but significant fraction remains as nuclear recoil energy. When a nucleus undergoes a transition from state E_e to state E_g by the emission of a photon, the conservation of momentum requires that the momentum of the atom, p_m, recoiling in one direction, is just equal and opposite to the momentum of the photon, p_γ, emitted in the opposite direction. The kinetic energy of the recoiling atom is E_R, so that for an atom of mass M and velocity v

$$E_R = 1/2\ Mv^2 = p_m{}^2/2M \tag{1}$$

Also, the momentum of the photon of zero rest mass is related to the energy by

$$E = p_\gamma c \tag{2}$$

so that

$$p_\gamma{}^2 = E_\gamma{}^2/c^2 \tag{3}$$

Since the two momenta must be equal, it follows that

$$E_R = E_\gamma^2/2Mc^2 \qquad\qquad (4)$$

A consequence of this conservation of momentum is that E_γ will be less than the transition energy, $E_t = E_e - E_g$, by E_R. Moreover, the energy required to populate the E_e state of an identical absorber (initially in state E_g) will be larger than E_t by the same amount E_R.

In the case of nuclear transitions, the spectral linewidth (Γ) is usually much smaller than the recoil energy, E_r, of the nucleus. For example, ^{121}Sb emits a γ-ray of energy 37.2 Kev and has an E_r of 6.124×10^{-3} ev and Γ of 1.304×10^{-7} ev. This effectively reduces the overlap between the line emitted by the source and that required to populate the corresponding transition in the absorber to a negligibly small value. Thus resonance will not occur under normal conditions.

In 1958, the German physicist R. L. Mössbauer[19,20] discovered the phenomenon of recoilless emission and resonant reabsorption of γ-rays while studying the 129 Kev line of ^{191}Ir. In order to reduce the natural overlap due to thermal excitation which still persists at room temperature, he cooled his source and absorber to 78°K. Instead of finding the expected decrease in resonance effect, Mössbauer observed a marked increase in the resonant absorption. Mössbauer realized that the large resonance overlap implied by this decrease in transmission resulted from an appreciable fraction of the emission and absorption events occurring without any recoil energy loss. This is possible because in some of the absorption and emission processes

the momentum is taken up by the entire crystal rather than the individual nucleus. Since E_R is inversely proportional to the mass (Eq. 4) for a given momentum, this energy becomes essentially zero when the mass is raised by a factor of about 10^{18} from that of a nucleus to that of a small crystal. In terms of the Debye theory of solids, this implies that the quantum jump does not involve contributions from the phonon spectrum of the matrix material and such recoil-free transitions are usually referred to as "no-phonon" events.

A detailed discussion of the basic physics of the Mössbauer effect can be found in a paper by Boyle and Hall[21] and a book by Fraudenfelder.[22]

In most cases, the emitting nuclei are in different chemical environments - compared to the absorbing nuclei - so that the nuclear energy levels are not identical and the exact energy match could not be achieved and reabsorption could not occur. In order to observe a resonance effect, it is necessary to impart a velocity to the absorber, relative to the source. This motion changes the energy of the incident quanta by the Doppler Effect so that at a certain velocity there is correspondence with the excitation energy of the nuclei in the absorber. For example, in a nuclear transition having a linewidth Γ, it is possible to shift the photon energy emitted by the source by Γ by imparting to the source a Doppler velocity v so that

$$v = \Gamma c / E_t \tag{5}$$

The Doppler velocity of the relative source-absorber motion which is required to shift the gamma ray energy by one line width for ^{121}Sb is $v = (1.304 \times 10^{-10}/37.2) \times 3.0 \times 10^{10} = 1.17$ mm/sec as compared to that of ^{57}Fe $= 0.0945$ mm/sec and ^{119}Sn $= 0.303$ mm/sec.

In this study a constant acceleration drive system was used to impart a constantly varying Doppler shift to the emitted γ-rays. A typical Mössbauer spectrum consists of the total number of events (counts) observed as a function of the relative velocity of the source and sample.

The profile of the resonance maximum obeys (ideally) the Lorentz relationship

$$I(E) = \text{constant}/[(E - E_0)^2 + 1/4\ \Gamma_{exp}^2] \qquad (6)$$

where E_0 is the Doppler energy at resonance maximum. Since the resonance line which is observed is a measure of the overlap of two lines of width Γ, the measured full width at half maximum is $2\Gamma_{nat} = \Gamma_{exp}$.

The real importance of the Mössbauer effect lies in the fact that it gives energy quanta of unprecedented precision. This precision allows us to detect very small changes in nuclear energy levels and to resolve hyperfine interactions which were previously totally excluded from experimental observation.

2. Magnitude of the Effect

The magnitude of the resonance effect depends on the fraction of all the detected events which are resonantly observed (f). More-

over, the magnitude of the resonance effect depends on the number of absorber nuclei in the optical path. ^{121}Sb has a high isotopic natural abundance (57%) and thus isotopic enrichment is not necessary. For low abundance Mössbauer nuclides such as ^{57}Fe (2.17%), ^{67}Zn (4.11%) and ^{170}Yb (3.03%), a marked increase in the magnitude of the effect can be obtained by enriching the absorbers, and enrichment becomes absolutely necessary when working with high molecular weight biological compounds.

The magnitude of the resonance effect also depends on the host lattice containing the source. Ideally this matrix should provide for narrow resonance lines, be easily prepared in high purity, be very stable and most importantly have a large recoil free fraction (f).

Ruby[7] used a $Ca^{121}Sn(Sb)O_3$ source with $f \approx 20\%$ at 300°K and $f = 60\%$ at 78°K. Another factor which determines the resonance effect magnitude is temperature.

Relative values of the resonance effect magnitude, which depend on the probability of recoil-free emission (f) and absorption (f') are strongly temperature dependent. The recoil-free fraction is related to the mean square amplitude of vibration $<x^2>$ by the equation

$$f = \exp(-4\pi^2<x^2>E_\gamma^2/h^2c^2) \tag{7}$$

where E_γ is the gamma ray energy involved. The value of $<x^2>$ for the atom involved in the emission or absorption can be derived from the Debye theory of specific heats.[23] In this model the Debye

temperature θ_D is defined as

$$\theta_D = h\omega_{max}/k \qquad (8)$$

where ω_{max} is the maximum oscillator frequency of the atom in the lattice from which

$$f = \exp[(-3E_R/2\theta_D k)(1 + \frac{2\pi^2}{3} \frac{T^2}{\theta_D^2})] \qquad (9)$$

when $T << \theta_D$. As $T \to 0$, the recoil-free fraction depends only on the ratio of the recoil energy E_R to the Debye temperature, so that substituting

$$E_R = E_\gamma^2/2Mc^2 \qquad (4)$$

we have

$$f = \exp(-3E_\gamma^2/4Mc^2k\theta_D) \qquad (10)$$

in the low temperature limit. As the temperature is increased, the term T^2/θ_D^2 becomes appreciably large and reduces the value of f by the factor e^{-T^2}. For most antimony compounds the Debye temperature is well below 300°K and thus the absorbers must be cooled down to at least 78°K and in many cases down to 4.2°K in order to observe a resonance effect.

3. Isomer Shift

The isomer shift, defined as the displacement from zero relative source-absorber velocity of the centroid of the resonance spectrum, is most closely related to the nature of the chemical environment of the resonant nuclei. It arises from the fact that the nucleus is not a point charge but occupies a finite volume of space, and, as a first

approximation, can be considered a spherical entity. As such, there is an interaction between the nucleus and the electrostatic field produced by all the extranuclear charges. Since the electronic environment of the nucleus is related to the chemical identity of the matrix in which the nucleus is embedded, the interaction between the nucleus and the electrostatic field can be related to the chemical nature of the material. A relationship between the isomer shift and the electron density at the nucleus can be simply derived as follows. To simplify the calculation, the difference between the electrostatic interaction of a hypothetical point nucleus and one of actual radius R, both having the same charge, is determined. A point nucleus of atomic number Z gives rise to an electrostatic potential at a distance r of

$$V = -Ze/r. \tag{11}$$

For a finite nucleus of radius R, the potential will be identical to that of a point nucleus for r > R, but equal to

$$V' = -Ze/r \mid 3/2 - r^2/2R^2 \mid \tag{12}$$

for r < R. An electron cloud of uniform density ρ, interacting with the nuclear charge will result in a perturbation energy of

$$E = \int_0^\infty \rho V 4\pi r^2 dr \tag{13}$$

in the hypothetical case and of

$$E = \int_0^\infty \rho V' 4\pi r^2 dr \tag{14}$$

in the actual case. The energy difference between the two is given
by the integral

$$\delta E = \int_0^\infty \rho(V' - V) \, 4\pi r^2 dr \qquad (15)$$

$$= 4\pi\rho Ze \int_0^R (3/2 - r^2/2R^2 - R/r)r^2 dr \qquad (16)$$

$$= 2/5 \; \pi\rho ZeR^2 \qquad (17)$$

Since the electron density at the nucleus is approximately large
only for s electrons, ρ can be approximated by $|\psi_s(0)|^2 e$, thus giving

$$\delta E = 2/5 \; \pi Ze^2 R^2 \; | \; \psi_s(0) \; |^2 \qquad (18)$$

This expression relates the electrostatic energy of the nucleus
to the radius, which generally is different for each energy level.
Observations, however, are made, not on the location of individual
nuclear levels, but on gamma rays resulting from transitions between
two such levels. The energy of the gamma ray represents the differ-
ence in electrostatic energy of the nucleus in two different states,
which in our model differ only in nuclear radius. Thus, the expression
for the change in energy of the gamma ray due to the nuclear electro-
static interaction is the difference of two terms like Eq. (18),
written for the nucleus in the ground and excited states

$$\Delta(\delta E) = \delta E_{ex} - \delta E_{gd} = 2/5 \; \pi Ze^2 |\psi(0)|^2 (R_{ex}^2 - R_{gd}^2) \qquad (19)$$

while $|\psi(0)|^2$ is assumed to remain constant. At this point the con-
tribution to δE from the point nucleus drops out.

In practise, $\Delta(\delta E)$ is not measurable directly, but can be
evaluated only with respect to a given source-absorber pair. Thus

$$\Delta\left|\Delta(\delta E)\right| = 2/5 \; \pi Z e^2 (R_e^2 - R_g^2)\{\left|\psi_s(0)\right|_a^2 - \left|\psi_s(0)\right|_s^2\} = \text{I.S.} \qquad (20)$$

This simplifies to

$$\text{I.S.} = 4\pi/5 \; Z e^2 R_g{}^2 (\delta R/R_g)\{\left|\psi(0)\right|_a^2 - \left|\psi(0)\right|_s^2\} \qquad (21)$$

where δR is the difference in nuclear radius of the excited and ground states. From this equation it is seen that the isomer shift is the product of a constant term $[4\pi/5 \; Z e^2 R_g{}^2]$, a nuclear term $\delta R/R$, and a chemical term $\{\left|\psi(0)\right|_a^2 - \left|\psi(0)\right|_s^2\}$. If the sign and magnitude of $\delta R/R$ is known, the electron density at the nucleus in the absorber and the source can be compared in a quantitative manner from measurements of the isomer shift.

The sign of $\delta R/R$ for [121]Sb is negative, i.e., the nuclear radius decreases on excitation from the ground 5/2 state to the excited 7/2 state. Thus the isomer shift has a negative dependence on the s electron density at the nucleus, i.e., as the "s" electron density increases the isomer shift decreases.

The isomer shift is the most important Mössbauer parameter due to its sensitive dependence on oxidation state. Experimentally, the fact that $\delta R/R$ is large for [121]Sb ($8.5 \pm 3 \times 10^{-4}$)[6] makes it easier to measure isomer shifts in antimony rather than say [119]Sn, in spite of the larger line width, since the I.S. for the two oxidation states are more widely separated. In Sb^{3+} we have an electron configuration $5s^2 5p^0$ while for Sb^{5+} we have the configuration $5s^0 5p^0$. Thus Sb(III) compounds have a higher "s" electron density and hence a more negative isomer shift than Sb(V) compounds. Isomer shifts in the range -11 mm/sec to -3 mm/sec have been found to be characteristic of Sb(III)

and shifts in the range +2 mm/sec to +12 mm/sec have been found to be typical of Sb(V) compounds (all shifts relative to InSb).

4. Quadrupole Splitting

If a nucleus is not spherical, and does not have a uniform charge density, effects appear which are higher order terms in the multipole expansion of the electrostatic interaction between nuclear charge and electronic environment. These effects lift the $(2I + 1)$ fold degeneracy, and the nuclear level will be split into $(I + 1/2)$ components having the same centre as the unsplit level. A nucleus with spin, I, greater than 1/2 is a non-spherically symmetric nucleus and has a quadrupole moment Q. An oblate (flattened) nucleus has a negative quadrupole moment while a prolate (elongated) one has a positive moment. The interaction of this quadrupole moment and the electric field gradient tensor lifts the degeneracy of the state. The presence of a non-zero field gradient at the nucleus is primarily determined by the symmetry of the electron distribution about the nucleus. This in turn is dependent upon the symmetry of the bonding about the atom of interest. In general, the presence of two mutually perpendicular axes of threefold or higher symmetry will result in a zero field gradient whereas in lower symmetries, quadrupole interactions will be observed. The field gradient can be specified by the three components $\partial^2 V/\partial x^2 = V_{xx}$, $\partial^2 V/\partial y^2 = V_{yy}$ and $\partial^2 V/\partial z^2 = V_{zz}$. These components are not independent, since they must obey the Laplace equation

$$V_{xx} + V_{yy} + V_{zz} = 0 \qquad (22)$$

in a region where the charge density vanishes.

The charge density of the s electrons does not vanish at the nucleus, but since the s electrons have a spherically symmetric distribution they do not contribute to the field gradient. Two independent components are chosen as V_{zz}, denoted eq, and η, the asymmetry parameter, defined by

$$\eta = V_{xx} - V_{yy}/V_{zz} \tag{23}$$

These components are usually chosen so that $|V_{zz}| > |V_{xx}| \geqslant |V_{yy}|$, making $0 \leqslant \eta \leqslant 1$. The interaction between the nuclear quadrupole moment, Q, and the gradient of the electric field, eq, is expressed by the Hamiltonian

$$H = \frac{e^2 qQ}{4I(2I-1)} [3I_z^2 - I(I+1) + \frac{\eta}{2}(I_+^2 + I_-^2)] \tag{24}$$

where I_+ and I_- are the shift operators.

Equation (24) has the eigenvalues

$$E_Q = \frac{e^2 qQ}{4I(2I-1)} [3m_I^2 - I(I+1)](1 + \frac{\eta^2}{3})^{1/2} \tag{25}$$

where the magnetic quantum number, $m_I = I, I-1, \ldots, -I$. A full derivation of these equations is given in a paper by Boyle and Hall.[21] Expression (25) contains only the second power of the magnetic quantum number m_I, which means that the states whose m_I differ only in sign remain degenerate. Unlike ^{57}Fe and ^{119}Sn whose $1/2 \rightarrow 3/2$ transition gives rise to two equally intense lines in the presence of an electric field gradient, ^{121}Sb, with a $5/2 \rightarrow 7/2$ transition, gives a more complex eight-line pattern. The energy level diagram for a quadrupole

split line in ^{121}Sb is illustrated in Figure 1. Moreover, the lines
are not of equal intensity. The expected intensities of the lines
are given by the squares of the Clebsch-Gordan coefficients of the
transition probabilities integrated over all angles. The relative
positions and intensities of the allowed transitions are presented
in Figure 1, for R = $Q^{121}(7/2)/Q^{121}(5/2)$ equal to 1.32.[24]

In practise these eight lines cannot be resolved because of
their large natural linewidths. The result is that the Q.S. affects
the shape of the resonance absorption so that when Q.S. occurs the
isomer shift is not at the maximum point in the absorption envelope
but at a point determined by the weighted average of all eight
transitions. Thus all Q.S. spectrum should be computer-fitted to an
eight-line quadrupole splitting pattern to obtain accurate Q.S. and
isomer shift parameters. In the case of ^{121}Sb, this inherent line
asymmetry is a very important parameter in ^{121}Sb Mössbauer work in
that the sign of the electric field gradient can be determined
readily by examining the shape of the spectrum. A change in sign
of the electric field gradient results in a marked change in the
transition probabilities of the eight lines causing a discernible
change in spectrum shape.

A positive Q.S. implies a negative electric field gradient
(since Q for ^{121}Sb is negative), indicating an excess of electron
density along the symmetry axis. An example of a positive Q.S. is
found in Sb_2O_3.[4] Trigonal bipyramidal R_3SbX_2[14] type compounds
show large negative Q.S. implying a greater electron density along
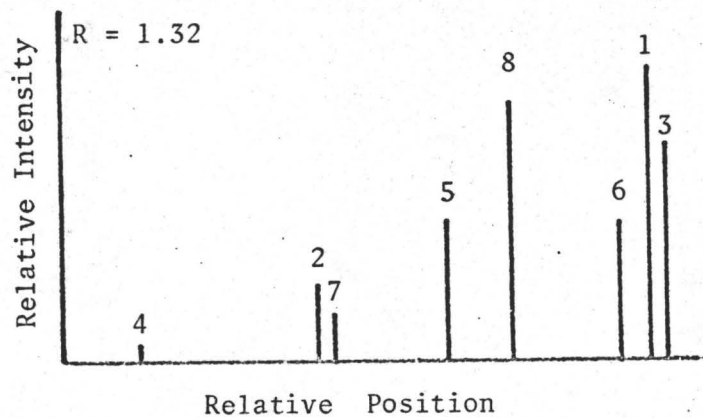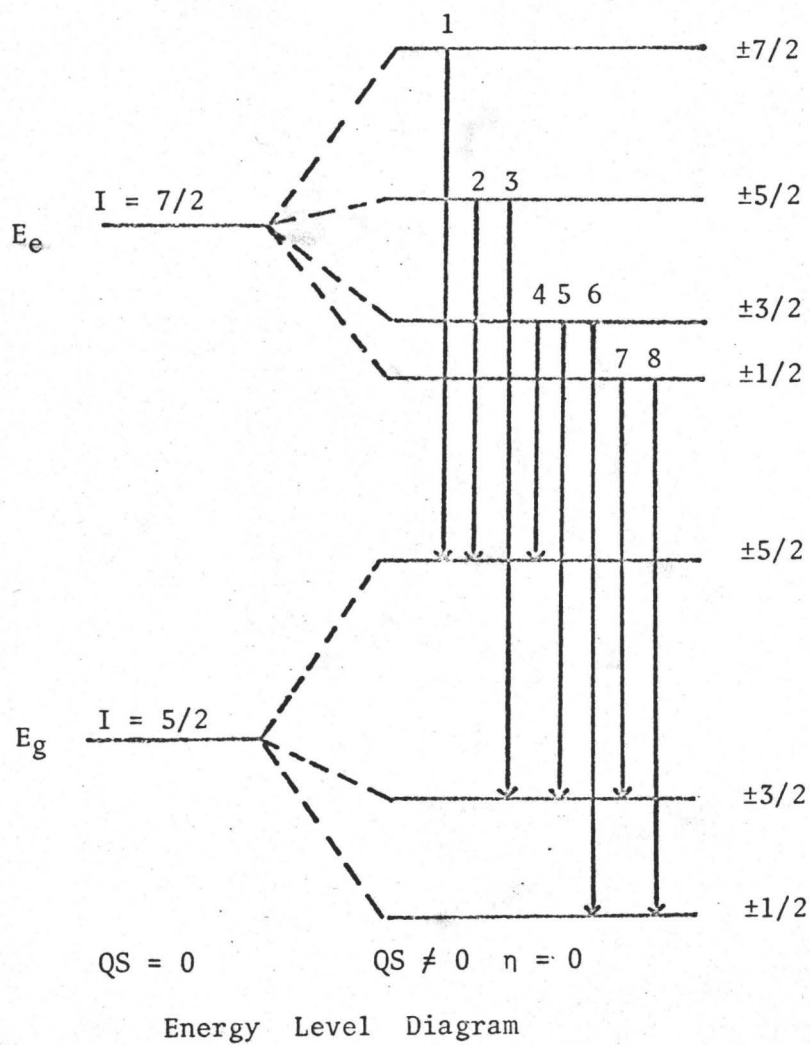the x and y direction than along the z axis.

Figure 1. ^{121}Sb Quadrupole Interaction.

5. Magnetic Hyperfine Interactions

In an asymmetric electric field, states with magnetic quantum numbers $+m_I$ and $-m_I$ occur at the same energy. This degeneracy can be removed by placing the Mössbauer nucleus in a magnetic field. This magnetic field may arise either internally, i.e., in a ferromagnetic material, or externally, generated by a magnetic device. Under these conditions, a nuclear Zeeman effect is observed in which each nuclear energy level is split into $2|m_I| + 1$ components. The energy of these levels is given by

$$E = -\mu H_m / I \qquad\qquad (26)$$

where μ is the nuclear magnetic moment and H is the hyperfine magnetic field. As in the case of isomer shifts and quadrupole interactions, the energy levels depend both on a nuclear factor μ, and an extra-nuclear factor, H. Transitions between these sub-levels are governed by the selection rules $\Delta m = 0, \pm 1$.

In the case of ^{121}Sb, a purely magnetic hyperfine interaction will cause the ground state of ^{121}Sb to split into six levels and the excited state into eight levels. Between these levels, the selection rules allow eighteen transitions.

To date only two magnetic hyperfine splittings have been observed in compounds of ^{121}Sb. These splittings occurred in the ferromagnetic materials MnSb at 4.2°K[5] and yttrium iron garnet at 100°K.[18] The experimentally observed spectrum in both cases constitutes a group of four prominent lines of about equal intensity and two pairs of weaker satellites on each side of the group, the

intensity of the outer lines of each pair being very low.

6. Line Width and Asymmetry

The width of the experimentally observed resonance line Γ_{exp} defines, to a large extent, the resolution of a resonance spectrum, and the factors which govern the magnitude of this parameter must be considered in the design of an optimum Mössbauer experiment. In an ideal resonance experiment, the value of Γ_{exp} is simply twice Γ_{nat}, the natural line width, which is given from the Heisenberg uncertainty principle as

$$\Gamma_{nat} = h/2\pi\tau \qquad (27)$$

where τ is the mean lifetime of the excited state. In practise, however, it is seldom possible to observe resonance lines as narrow as $2\Gamma_{nat}$, due to broadening effects such as nonhomogeneity of chemical environments of the resonant atoms in source and/or absorber, finite absorber thickness, geometric effects, thermal effects and the presence of hyperfine structure due to extranuclear field effects. Nonetheless, the resonance line width which is observed with a standard absorber is, in addition to the magnitude of the resonance effect, the most reliable measure of the quality of a Mössbauer source. In the case of ^{121}Sb the Γ_{exp} is 2.1 mm/sec which is ten times greater than Γ_{exp} for ^{57}Fe.

Quadrupole split lines sometimes give rise to lines of unequal intensity. Two factors can cause this effect.

The presence of preferential orientation of the absorber crystallites so that non-random orientations of a unique crystal axis with

respect to the source-detector axis can cause line asymmetry in iron and tin spectra.

The origin of the non-equivalence of the line intensities lies in the angular dependence of this intensity, which differs for different m_I values. The maximum difference in intensity occurs when the symmetry axis is parallel to the optical axis. However, for a finely-powdered absorber material where the crystal orientations are random, the line intensities should be of equal value. This factor is very much more complex for the [121]Sb case than for the [57]Fe or [119]Sn cases since the eight quadrupole split lines are not of equal intensity to begin with.

A further contribution to line asymmetry arises from the angular anisotropy of the probability of emission (or absorption) of a quantum in a recoil-free transition. This is commonly referred to as the Goldanskii effect,[25,26] but was originally mathematically formulated by Karyagin.[27] The probability of a recoil-free transition is related to the mean square vibrational amplitude x^2 by the equation

$$f = \exp(-4\pi^2 <x^2>/\lambda^2) \qquad (28)$$

where λ is the wavelength of the radiation and the value of $<x^2>$ is averaged over the transition lifetime.

Since $<x^2>$ is dependent on the strength of a chemical bond in a given direction, there will be an angular dependence of the recoil-free fractions for emission and absorption leading to different angular dependencies and thus unequal line intensities. In cases where there is a large asymmetry in the chemical bonding, this line

asymmetry is especially pronounced and this asymmetry persists even when there is random orientation of the crystal axes with respect to the optical axis.

In ^{121}Sb the Goldanskii-Karyagin factor was noted to be less than one for the compounds R_3SbX_2[15] implying larger amplitudes of vibration in the axial direction as compared to the equatorial plane directions.

CHAPTER III

Experimental

1. Preparation of Antimony Chalcogenides, Oxides and Phosphate

Sb_2O_5: $SbCl_5$ was added to 25 times its weight of cold water and after two hours, the white precipitate was filtered, washed with cold water and dried at 275°C.[28] (Calc'd: Sb, 75.30; Found: Sb, 70.97)

Sb_2O_4: Antimony(V) oxide was ignited in a Pt crucible at 800-900°C for about two weeks.[28] It was also prepared by Vogel's method[29] i.e., by reacting Sb_2S_3 with fuming nitric acid and igniting at 800° for one hour. The former compound did not dissolve in strong acid while the latter compound dissolved easily in conc. HCl. (Calc'd: Sb(III), 39.59; Sb (total), 79.18; Found: Sb(III), 41.29; Sb (total), 78.10)

Sb_2O_3: A commercial sample (Baker and Adamson) was used.

$SbPO_4$: Sb_2O_3 was dissolved in conc. H_3PO_4 and filtered through a sintered glass filter. Cold water was then added and the solution allowed to stand for a few hours whereupon a white powder came out of solution. (Calc'd: Sb, 56.20; Found: Sb, 56.00)

Sb_2S_3: A solution of 10 g of $SbCl_3$ in 400 ml of dilute (150:250) hydrochloric acid was prepared. Then H_2S was bubbled through the solution for fifteen minutes causing a fine orange precipitate of Sb_2S_3 to form. This precipitate was filtered, washed with water and then oven-dried for about four hours at 120°, whereupon the precipitate turned black.[28] (Calc'd: Sb, 71.68; Found: Sb, 71.60)

22

Sb_2Se_3 and Sb_2Te_3:   These compounds were purchased from Alpha
Inorganics, Inc.

$Na_3SbS_4 \cdot 9H_2O$: This compound was prepared by mixing Sb_2S_3, 20% NaOH
and powdered sulphur, and boiling for one-half hour. The solution
was filtered and evaporated until crystallization began. Large,
bright yellow tetrahedral crystals were then separated and dried.[28]

Sb_2S_5: The common literature preparations[30] of this material such
as treating an antimony(V) solution with H_2S or by acid decomposition
of sodium thioantimonate(V) nonahydrate were repeated. Also a
commercial sample of Sb_2S_5 was obtained from Alpha Inorganics Inc.

2. Preparation of Chloro Complexes of Antimony

These compounds were kindly provided by E. Martineau and J. B. Milne
from the University of Ottawa. The hexachloroantimonate(III) compounds
R_3SbCl_6 (R = Cs, NH_4, K) were prepared from antimony trichloride and
the monochloride in liquid sulphur dioxide as described by Martineau
and Milne.[31] Ammonium pentachloroantimonate(III) was made from
ammonium chloride and antimony trichloride by the method of Edstrand
and coworkers.[32] The black rubidium hexachloroantimonate(IV) and
the brown compound, $Rb_{16}Sb_6Cl_{36}$ (calc'd: Cl, 38.24; Sb(III), 18.04;
found: Cl, 37.88; Sb(III), 17.06) were prepared according to the
literature.[33] The hexamine cobalt(III) hexachloroantimonate(III)
was made according to the procedure of Barrowcliffe and coworkers.[34]
Rubidium hexachloroantimonate(V) was prepared from a 1:1 stoichiometric
ratio of rubidium chloride and antimony pentachloride in liquid sulphur
dioxide, contained in a vessel fitted with a break-seal, for removal of

the solvent after the reaction was complete. Rubidium chloride

(B.D.H.) was recrystallised once from water, and antimony pentachloride

(Baker and Adamson) was distilled under high vacuum three times.

Rubidium chloride was soluble in liquid sulphur dioxide containing

antimony pentachloride and the hexachloroantimonate(V) was recovered

by removal of all the solvent. The product did not contain any

sulphur and an X-ray powder photograph showed no lines for RbCl.

(Calc'd: Cl, 50.65; Found: Cl, 50.50). The ammonium hexabromo-

antimonate(IV) was prepared by the method given by Brauer.[28]

3. Preparation of the Fluoro Anions of Antimony

Attempts were made to prepare all of the compounds reported by

Bystrom and coworkers according to their procedures.[35-39] These

methods did not always prove successful. For example, all attempts

to prepare KSb_4F_{13} gave KSb_2F_7 and it is very unlikely that the

former compound exists. It is interesting to note that Bystrom

and Wilhelmi provide no analytical data for this compound.

KSb_2F_7: Several procedures yielded samples of this compound. Dis-

solution of Sb_2O_3 and K_2CO_3 in a 2:1 mole ratio in excess aqueous

HF and allowing the solution to cool gave crystals of KSb_2F_7. This

compound was also obtained from the attempted preparation of KSb_4F_{13}

and from Bystrom's procedure for obtaining K_2SbF_5 except that the

residue was recrystallised at room temperature from aqueous HF.

(Calc'd: Sb, 58.70; Found: Sb, 59.00).

$NaSbF_4$: This was prepared by dissolving Sb_2O_3 and Na_2CO_3, in a 1:1

mole ratio, in excess aqueous HF, evaporating to dryness and re-

crystallising from water at room temperature. Clear colourless crystals were obtained. (Calc'd: Sb, 55.10; Found: Sb, 54.30).

$KSbF_4$: This was prepared in an analogous manner to the sodium salt yielding a white powdery compound. (Calc'd: Sb, 51.40; Found: Sb, 52.10).

K_2SbF_5: This compound was produced while attempting to prepare K_3SbF_6 by dissolving Sb_2O_3 and K_2CO_3 in a 1:3 mole ratio in excess aqueous HF. The solution was evaporated to dryness and the residue recrystallised twice from water at room temperature to give clear colourless crystals. (Calc'd: Sb, 41.30; Found: Sb, 41.00).

$KSbF_6$ was obtained from Ozark-Mahoning Co. and used without further purification.

$CsSb_2F_{11}$ was kindly supplied by Dr. P. A. W. Dean formerly of this Department.

4. Complex Antimony Fluorides and Fluorosulphates

The compounds $Sb^ISb_2F_{11}$, Sb^IAsF_6, Sb^ISO_3F, $SbF_3 \cdot SbF_5$ I (Calc'd: Sb(III), 30.78; Sb (total), 61.56; Found: Sb(III), 31.21; Sb (total), 62.51), $SbF_3 \cdot SbF_5$ II and $SbF_3 \cdot AsF_5$ were kindly provided by P. A. W. Dean, formerly of this Department. $Sb(SO_3F)_3$ was provided by O. C. Vaidya and $SbF_3 \cdot SbF_5$ III by B. Cutforth both of this Department. Antimony metal (99.7% pure) was obtained from Fisher Scientific Co.

5. Antimony-Containing Minerals

The three antimony-containing minerals Nadorite, Tetrahedrite, and Boulangerite were purchased from Filer's Co.

6. Method of Analysis

The percentage of antimony in the above compounds was determined by titration with standard iodine.[29] Sodium bicarbonate was added to remove the hydriodic acid formed. To prevent precipitation of basic salts as the solution was neutralized, tartaric acid was added forming the soluble antimonyl tartrate complex, $SbOC_4H_4O_6^-$, which is completely oxidized by iodine. The indicator used was a freshly prepared starch solution. The end point was realised when the originally colourless solution turned a faint blue colour which persisted for 30 seconds.

For the case of Sb(V) compounds, the antimony was first reduced to Sb(III) with red phosphorous and then titrated as above.

7. Mössbauer Apparatus

The Mössbauer spectra were recorded with an Austin Science Associates model S3 drive system, used in conjunction with a Victoreen PIP 400A multichannel analyzer operating in the multiscalar mode. The block diagram, Figure 2, illustrates the elements of the Mössbauer spectrometer. The power supply was an ORTEC 401A Modular System Bin. The gamma ray source was 500 micro Curie $Ba^{121m}Sn(Sb)O_3$ obtained from New England Nuclear Corp. The escape peak of the 37.2 Kev gamma rays was detected by a $Xe-CO_2$ (1 atm.) gas-filled proportional counter, model CSP-400, obtained from Austin Science Associates operating at 2000 volts. This detector unit included a close coupled field effect transistor preamplifier. Power for the detector unit was supplied by a DC regulated power supply, model 2K-10, from Power Designs Pacific, Inc.
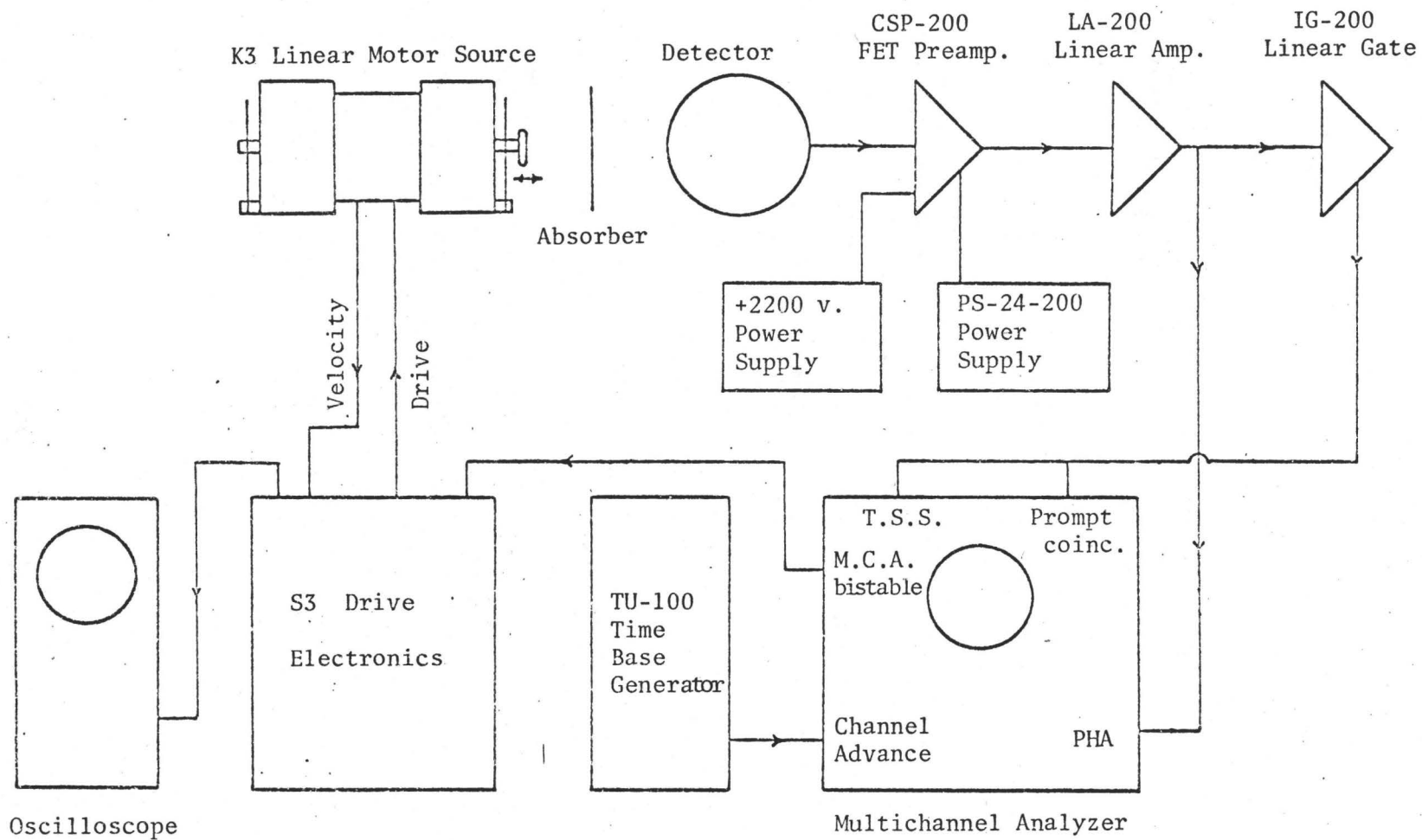
Figure 2.   Mössbauer Spectrometer - Block Diagram

The source is vibrated with constant acceleration. The velocity, and hence the gamma ray energy, varies linearly with time in a triangular mode. This triangular waveform was monitored on an oscilloscope providing a check on the linearity of the waveform. The resultant Mössbauer spectrum consists of a plot of count rate versus velocity. The sense of the constant acceleration motion is controlled by the 400 channel multiscaling M.C.A., and has opposite sign in alternate halves of the memory. Consequently, mirror image spectra appear in the memory halves, one spectrum being counted during intervals of increasing velocity and the other during intervals of decreasing velocity. Invariably there are other radiations emitted by the source which may interfere with the desired ray. For [121]Sb the spilldown from the 24 Kev X-ray causes the greatest interference. Thus it is essential that an energy selective device be used to ensure that only the desired gamma ray will be counted. The preamplifier and linear amplifier amplify and shape the resulting pulses. The voltage levels in the single channel analyzer can be set such that the window sits exactly on the required gamma ray. The signal from the single channel analyzer is counted and stored as information in the memory bank of the M.C.A., whose channel address varies in synchronism with the source velocity. A crystal controlled time base generator provides the signals for the address advance. The square wave from the M.C.A. is converted by an integrator in the drive electronics to a triangular waveform which controls the velocity drive. The antimony spectra were recorded with the source and detector as close as possible (approx. 10 cm) to maximise the count rate. The count rate for antimony was

quite low ranging from approximately 150 to 400 counts per channel
per hour. The antimony samples were all cooled to liquid nitrogen
temperatures. The spectra were accumulated for a minimum of two
days and sometimes for as long as seven days depending on the quality
of the spectra. Samples generally contained 10-40 mg Sb/cm^2 and were
held in 3.8 cm^2 holders either as a compressed powder or mixed with
grease.

8. Treatment of Data

Spectra were printed out as counts per channel on a Teletype
paper tape punch. This information was then converted to punched
card form. Initially the peaks were fitted to Lorentzian line shapes
using an iterative least squares method. The spectra were then
folded about the centre thus combining the two mirror halves using
the same program as above by calling the FOLD SUBROUTINE. If the
spectra proved to be non-Lorentzian in shape they were then fit by
another computer program, MOSFIT, to an eight-line quadrupole split-
ting pattern. In this program the relative intensities of the lines
were taken from the Clebsch-Gordan coefficients, the ratio of quadru-
pole moment of the excited state to the ground state was taken as
1.34[15] and the asymmetry parameter, η, assumed to be zero. The
drive velocity was calibrated using a standard iron foil with a
Pd (^{57}Co) source. All isomer shifts are quoted with respect to the
compound InSb at liquid N_2 temperature which gives a sharp symmetrical
single line. The error in isomer shift ranges from 0.4 mm/sec to
0.06 mm/sec while the error in quadrupole splitting varies from 0.6

mm/sec to 1.8 mm/sec. The error in the quadrupole splitting measurements were greater than the above limit in cases where the spectra were of low intensity and/or poorly resolved and also if the splitting was very small as in the case of symmetric six coordinate Sb(V) species.

CHAPTER IV

Results and Discussion

1. Antimony Chalcogenides, Oxides and Phosphate

The data for these compounds are summarised in Table I. Except for $SbPO_4$, the absorption envelopes have not been fitted to the eight-line quadrupole splitting pattern. However, the isomer shifts can be obtained reasonably accurately to yield useful chemical information. The shifts fall into two groups, namely those at very negative velocities typical of Sb(III) and those at more positive velocities, +2.9 mm/sec, and above, characteristic of Sb(V).

In the Sb_2X_3 series there is a considerable change to more negative velocities from oxygen to tellurium, indicating an increase in "s" electron density at the antimony nucleus, thus closer approximating the bare Sb^{3+} in the Sb_2Te_3 case. This agrees with the structures as far as they are known,[40,41] with the telluride having a more ionic lattice. Antimony(III) sulphide and selenide are isostructural, each consisting of hexagonal rings condensed to form long chains.[41] Within each structure there are two different antimony sites. For example, in Sb_2S_3 one antimony has three sulphurs at 2.50 Å and no others closer than 3.14 Å, while the other antimony has one sulphur at 2.38 Å, two at 2.67 Å, and two at 2.83 Å. Each site will give rise to a separate eight-line quadrupole split pattern which cannot be resolved, thus precluding a meaningful analysis in terms of quadrupole splitting and asymmetry parameters for each site. The

31

TABLE I

Mössbauer Data for the Chalcogenides, Oxides and Phosphate

Compound	Isomer Shift (mm/sec)	Quadrupole Coupling Constant (e^2qQ) (mm/sec)	% Absorption
Sb_2O_3	-3.0 ± 0.1	+18.8 ± 0.4 [6]	9
Sb_2S_3	-6.0 ± 0.2		7
Sb_2Se_3	-6.0 ± 0.4		5
Sb_2Te_3	-6.7 ± 0.2		3.5
$Na_3SbS_4 \cdot 9H_2O$	+2.9 ± 0.1		4
Sb_2O_5	+8.7 ± 0.3		9
Sb_2O_4	+8.9 ± 0.2		9
	-5.9 ± 0.2	+16.4 ± 0.6 [12]	7
$SbPO_4$	-6.0 ± 0.1	+18.4 ± 0.7	9.6

isomer shifts reported for these two compounds are therefore average shifts for the two kinds of antimony sites present (Figure 3a). Antimony(III) telluride, however, has the face-centred cubic Bi_2Te_3 structure with only one type of Sb site.[41] Unfortunately, the interatomic distances in Sb_2Te_3 are not known but, by analogy to Bi_2Te_3, each antimony should have three tellurium near-neighbours and three more distant in the five layer sandwich, resulting in six coordination. If the antimony 5s electron pair is also stereochemically active a quite distorted structure would result giving rise to an asymmetric Mössbauer absorption as illustrated in Figure 3b.

The nature of antimony pentasulphide was unknown.[40] The various samples prepared as described in Chapter II together with the commercial sample of "Sb_2S_5" gave, in each case, a Mössbauer spectrum consisting of only one absorption at -6.0 mm/sec, clearly in the Sb(III) region of the spectrum. No resonance due to Sb(V) could be detected. Furthermore, an examination of the Sb-S phase diagram[42] shows no evidence for compound formation at the 2Sb:5S composition. There appears to be no evidence for the existence of the "pentasulphide" of antimony. During the course of this investigation Long and his coworkers[11] came to similar conclusions. That the composition for "Sb_2S_5" is not stoichiometric is probably due to the substitution of polysulphide ions for sulphide ions in varying amounts. However, Sb(V) can exist coordinated by sulphur in the salt, $Na_3SbS_4 \cdot 9H_2O$. This had been prepared earlier and the antimony found to be tetrahedrally coordinated by sulphur.[43] The symmetrical

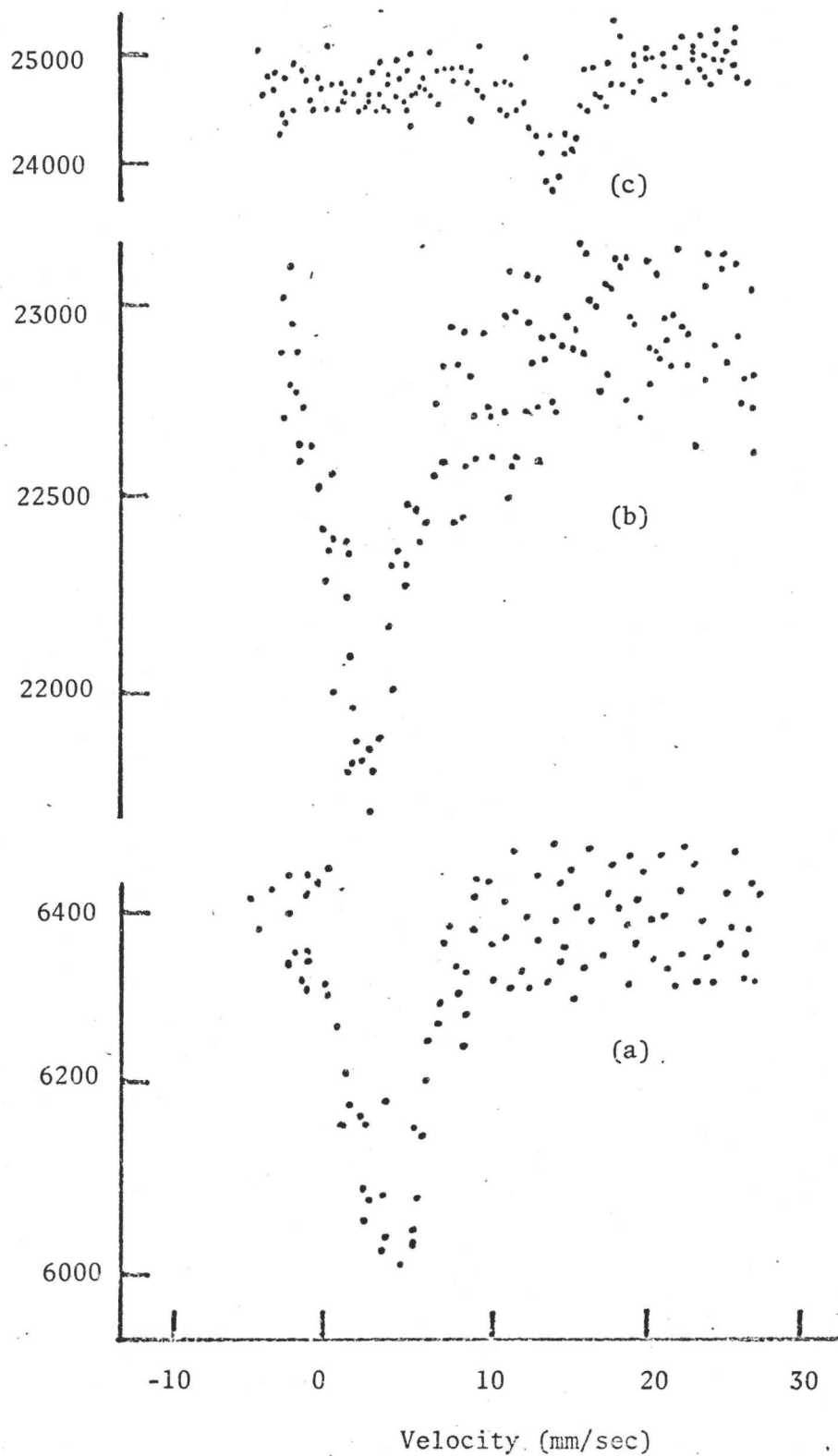Figure 3. Mössbauer Spectra: (a) Sb_2S_3, (b) Sb_2Te_3, (c) $Na_3SbS_4 \cdot 9H_2O$

Mössbauer absorption obtained for this compound (Figure 3c) is con-sistent with this structure. The isomer shift of +2.9 mm/sec is the least positive yet reported for an inorganic compound of Sb(V), being outside the limits set by Long,[12] and indicates considerable covalent character in the Sb-S bonds.

The data reported here on Sb_2O_5, Sb_2O_3 and Sb_2O_4 agree well with the literature values.[6,12] The spectrum for Sb_2O_4 showed two well-resolved peaks, one in the antimony(III) region of the spectrum, the other in the antimony(V) region, thus eliminating the possibility of an antimony(IV) oxidation state.

Skapski and Rogers[44,45] solved the crystal structures of both the α and β forms of Sb_2O_4. In both forms of Sb_2O_4 the Sb(V) atoms are found in layers, each Sb(V) being at the center of a slightly distorted octahedron of oxygen atoms. On the other hand, the Sb(III) atoms form columns between the layers with each Sb(III) having two oxygens at 2.032 Å and two at 2.218 Å.

The isomer shift of the absorption in the Sb(V) region of Sb_2O_4 (+8.9 ± 0.2 mm/sec) is virtually the same as that for antimony(V) oxide (+8.7 ± 0.3 mm/sec). Since the Sb(V) in Sb_2O_4 is at the center of a distorted octahedron of oxygens,[44,45] it seems reasonable to suppose that the antimony in antimony(V) oxide is probably also six coordinate. The analytical data for antimony pentoxide reveals a lower antimony content than expected for the Sb_2O_5 composition. This evidence suggests that Sb_2O_5 does not exist in pure form but is always somewhat hydrated.[28]

The crystal structure of $SbPO_4$[46] shows that the Sb(III) has a

one-side coordination to four oxygen atoms with Sb-O distances between 1.98 Å and 2.19 Å. A comparison of the corresponding angles and bond distances with the Sb(III) site in Sb_2O_4 shows no large differences, and as seen from the angles (∿90°) the influence of the inert pair is apparent in both cases. This similarity in structure is reflected in the close agreement in the Mössbauer parameters (Table I). It should be noted that for both Sb_2O_4 and $SbPO_4$ the isomer shifts in the Sb(III) region (-5.9 ± 0.2 and -6.0 ± 0.1 mm/sec, respectively) differ from the experimental value for Sb_2O_3 (-3.0 ± 0.1 mm/sec).

The more negative isomer shifts for Sb_2O_4 and $SbPO_4$ indicates a higher "s" electron density at the antimony nucleus in these compounds compared with that in Sb_2O_3. This could be due to the change in coordination number about the antimony. In Sb_2O_3 each antimony is surrounded by three near-neighbour oxygens at 2.0 Å in a pyramidal arrangement with three more distant oxygens at 2.9 Å together forming a distorted octahedral environment about the antimony.[47]

Various explanations have been offered for the difference in isomer shift between the Sb(III) sites in Sb_2O_4 and Sb_2O_3.[12,24] Long and coworkers[12] attribute the increased "s" electron density in Sb_2O_4 as being due to either a donation of electron density to the antimony from the "extra" oxygen in its coordination sphere, or due to less electron withdrawal by the two nearer oxygens in Sb_2O_4 compared to the three oxygens about Sb in Sb_2O_3. Stevens and Bowen[24] have suggested that since the two closest neighbours in Sb_2O_4

are at an angle of ∿90° to one another, there is little or no "s" character to these bonds. The next two nearest neighbours are

more distant, indicating weaker bonds which perhaps also have some d-character. The overall effect results in an increased "s" electron density at the Sb(III) nucleus. Neither of these groups consider the effect of the next nearest neighbours in Sb_2O_3 where there are three additional oxygens at 2.9 Å. While the interaction with these oxygens is obviously weak it could help reduce the "s" electron density by withdrawing charge from the nucleus.

2. Chloro Complexes of Antimony

The Mössbauer data are summarised in Table II. The spectra obtained had absorptions varying from 1-6%, and, apart from $(NH_4)_2SbCl_5$ appeared as symmetrical lines (Figures 4 and 5). For this reason the data, except $(NH_4)_2SbCl_5$, were fitted to single Lorentzian line shapes. This certainly seemed justified for compounds 1-3 and 8 in Table II, which have linewidths which were natural (2.1 mm/sec) or only slightly greater. The remaining absorptions were somewhat broader, particularly that of $(NH_4)_2SbCl_5$ which was clearly asymmetric, indicating the presence of an appreciable electric field gradient at the antimony nucleus in this compound. The spectrum of this compound was fitted to an eight-line quadrupole split pattern and a quadrupole coupling constant of +11.2 mm/sec was obtained. This result is expected in view of the published crystal structure.[32] The antimony has five chlorines in a square pyramidal arrangement about it, with the lone pair occupying what would normally be the sixth coordination position of an octahedral arrangement. This is clearly a non-cubic structure with excess electron density along the axis of symmetry giving rise to the positive and

TABLE II

Mössbauer Data for the Chloro Complexes of Antimony

	Compound	Isomer Shift (mm/sec)	Line Width (mm/sec)	Q.C.C. (e^2qQ) (mm/sec)
1.	$Rb_4Sb_2Cl_{12}$	-11.1 + 5.75	2.2 2.4	
2.	$Rb_{16}Sb_6Cl_{36}$	-10.6 + 6.2	2.8 4.1	
3.	$[Co(NH_3)_6]SbCl_6$	-11.2	3.1	
4.	K_3SbCl_6	- 9.7	3.5	
5.	Cs_3SbCl_6	- 9.6	3.6	
6.	$(NH_3)_3SbCl_6$	- 8.7	4.3	
7.	$(NH_4)_2SbCl_5$	- 6.5	4.4	+11.2 ± 1.8
8.	$RbSbCl_6$	+ 5.8	2.8	
9.	$(NH_4)_4Sb_2Br_{12}$	- 8.7 + 2.8	- -	

The above isomer shifts are accurate to 0.2 mm/sec.
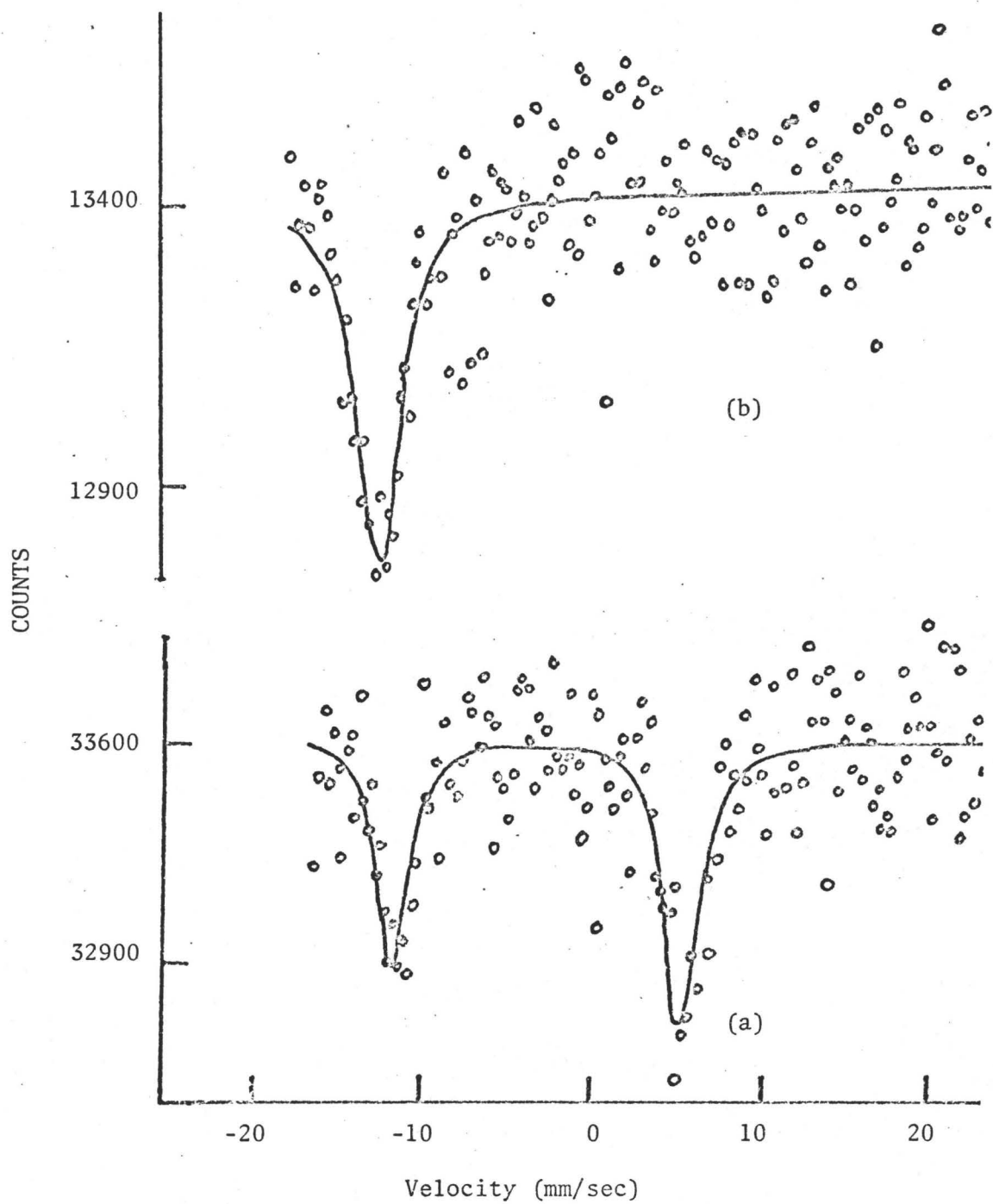
Figure 4. Mössbauer Spectra: (a) $Rb_4Sb_2Cl_{12}$, (b) $Co(NH_3)_6SbCl_6$.
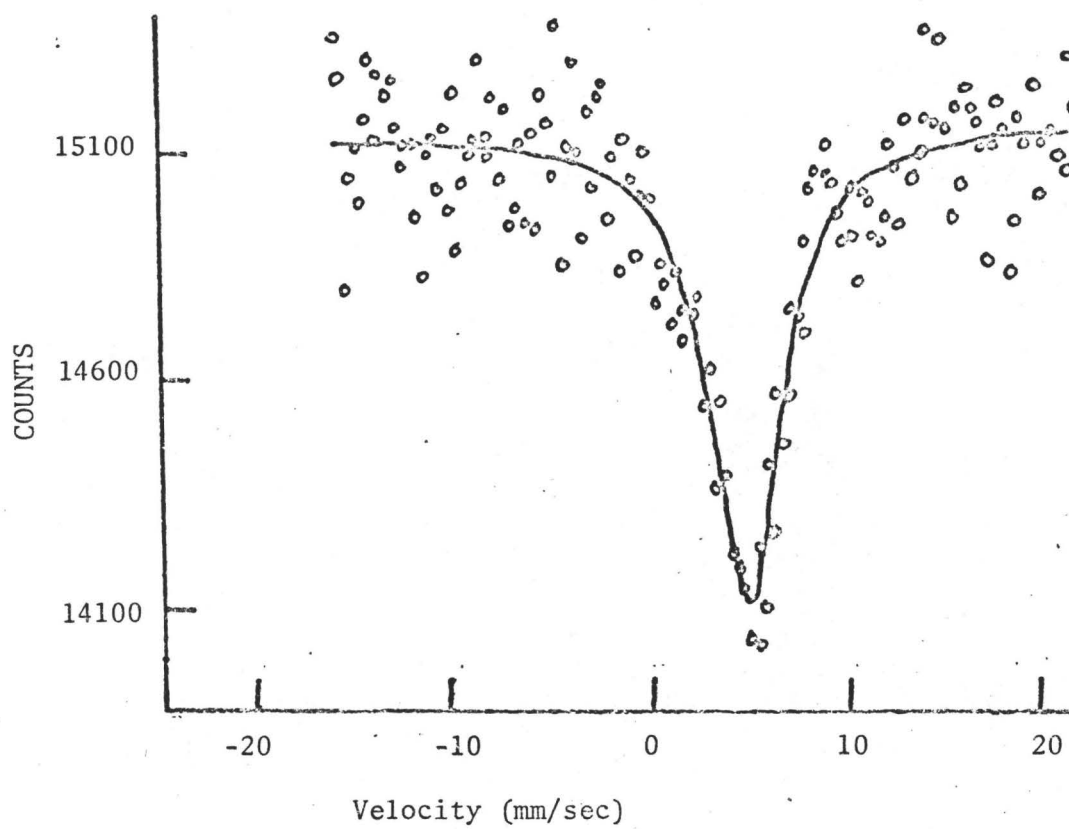
Figure 5. Mössbauer Spectrum: $RbSbCl_6$.

fairly large quadrupole splitting.

Recently a crystal structure of $(NH_4)_2SbBr_6$ has been published[48] which is consistent with the evidence summarised by Robin and Day[49] that this compound is in reality $(NH_4)_4Sb(III)Sb(V)Br_{12}$. This formulation has been confirmed by Long and his coworkers[50] in a preliminary report of their Mössbauer data. Our results are also in agreement with this formulation. The spectrum showed two resonance absorptions, one at -8.7 mm/sec which is characteristic of Sb(III) and the other at +2.8 mm/sec clearly in the Sb(V) region. Two resonance absorptions were obtained for $(Rb_2SbCl_6)_n$ (Figure 4a), and $(Rb_8Sb_3Cl_{18})_n$, thus establishing the presence of both Sb(III) and Sb(V) in these compounds also.

The black salt $(Rb_2SbCl_6)_n$ which had been prepared by Weinland and Schmid,[33] and Jansen,[51], has the two ^{121}Sb absorptions in a 1:1 ratio and is clearly analogous to the ammonium hexabromoantimonate (III) (V) where n = 2 and should be formulated as $Rb_4Sb(III)Sb(V)Cl_{12}$. $(Rb_8Sb_3Cl_{18})_n$ has an Sb(III) resonance which is much more intense than that in the Sb(V) region but the poor quality of the spectrum precludes any accurate area information. The best estimate from the Mössbauer spectrum indicates that the absorptions are in a ratio >> 2:1. This, taken together with the analytical data and the results of previous workers[33,52] finds n=2 leading to a formulation of $Rb_{16}[Sb(III)]_5Sb(V)Cl_{36}$ for this compound.

The isomer shift for the Sb(V) absorption in $Rb_4Sb_2Cl_{12}$ and $Rb_{16}Sb_6Cl_{36}$ is in good agreement with that for $RbSb(V)Cl_6$ (Figure 5). The width of these absorptions for $Rb_4Sb_2Cl_{12}$ and $RbSbCl_6$ indicates that the Sb(V) is in a symmetrical environment. It also seems pro-

bable that the Sb(V) site in $Rb_{16}Sb_6Cl_{36}$ is also cubic, in spite of the apparent width. This spectrum gave an absorption of <1% in this region so that the width obtained may not be very meaningful. Mössbauer shifts for other hexahaloantimony(V) compounds have been reported by Ruby[6] and others.[8,24] Our values for the $Sb(V)Cl_6^-$ anions are in substantial agreement with that reported for $HSbCl_6 \cdot xH_2O$[8] and are less positive than that of SbF_6^-.[6,8] The isomer shift increases from +2.8 mm/sec, for the $Sb(V)Br_6^-$ anion, through +5.75 mm/sec for $Sb(V)Cl_6^-$, to +10.6 - +12.3 mm/sec for the $Sb(V)F_6^-$ reflecting the effect of increasing ligand electronegativity. An essentially ionic Sb^{5+} can be considered present in the SbF_6^- salts with increasing covalent character to the Sb-X bonds as the electronegativity decreases from F through Cl to Br.

The isomer shifts for the Sb(III) species proved to be quite interesting. These shifts are the most negative yet reported. Stevens and Bowen[24] have summarised the attempts at estimating the isomer shifts for a bare Sb^{3+}.

From a plot of isomer shift versus quadrupole splitting for some Sb(III) compounds they predict an isomer shift of -10.6 ± 0.3 mm/sec for Sb^{3+}, i.e., the shift for an antimony(III) in which there is no "s" character in the bonds to the ligands. Compounds 1-3 (Table II) have resonance absorptions ranging from -10.6 to -11.2 mm/sec for the Sb(III) species, and the narrow linewidths suggest very symmetrical antimony environments.

Taken together, these facts indicate that the Sb is not using the 5s electron pair in bonding to the six halogen ligands. Thus,

in this case, we have reached an essentially ionic Sb^{3+} situation in these compounds and confirms the estimated shift for Sb^{3+} made by Stevens and Bowen.[24]

The shifts for the other $[Sb(III)Cl_6]^{3-}$ species are somewhat less negative and it is interesting to note that the trend to more positive values is reflected by an increase in line width. This would seem to indicate an increasing participation of the 5s electron pair in the bonding from the $[Co(NH_3)_6]^{3+}$ salt to the NH_4^+ salt. Complete participation of the 5s pair would result in a seven coordinate species with accompanying electric field gradient and the resulting antimony Mössbauer absorption would be expected to be broad and asymmetric. The isomer shift for such a species might approach that for $[SbCl_5]^{2-}$ in which the 5s pair is stereochemically active and the absorption is broad and asymmetric. The data indicate that the Sb(III) in compounds 1-3 is in a symmetric environment. In K_3SbCl_6 and Cs_3SbCl_6 a more distorted environment is found with $(NH_4)_3SbCl_6$ deviating further from O_h symmetry. Raman studies on these compounds (3-6) indicate that the $SbCl_6^{3-}$ anions are distorted in the solid state but not in solution.[31] Distortions in the crystal lattice produced by an asymmetric distribution of cations would give rise to an electric field gradient at the antimony nucleus to produce a quadrupole splitting of the resonance lines and this would produce a broadening of the absorption envelope. Such an effect would not produce a change in isomer shift. Since both isomer shift and the resonance line width are changing, the distortions produced by the various cations are affecting the octahedral geometry about the central

antimony. This causes the 5s electron pair to become involved in the bonding scheme and produce the observed changes in isomer shift. However, conclusions based on the line width parameter alone would be misleading since this parameter is, unlike isomer shift, difficult to determine accurately. Furthermore it is affected by the sample thickness and our spectra were not all recorded with the same density of Sb/cm^2. The Mössbauer parameters for the $[Co(NH_3)_6]^{3+}$ salt (Figure 4b) would indicate that the Sb is in a symmetric environment and the Raman data can be explained by the reduced site-symmetry as suggested by Martineau and Milne.[31]

Very recently Adams and Downs[53] presented evidence which indicated that the $SbCl_6^{-3}$ ion in $[Co(NH_3)_6][SbX_6]$ salts have a symmetrical environment. The very low isomer shift for this compound is also consistent with the estimated Sb-Cl bond length of 2.52 Å which is longer than the mean Sb-Cl distance in Rb_2SbCl_6.[48] Once again, the effect of ligand electronegativity is evident, this time on the Sb(III) resonance in the M_2SbX_6 salts, where the chloride has a more negative isomer shift than the bromide.

Ruby[7] has compared the isomer shift parameters for compounds of ^{121}Sb with the analogous compounds of ^{119}Sn. A plot of the ^{121}Sb isomer shifts versus the ^{119}Sn isomer shifts gives a straight line correlation (Figure 6). The ^{121}Sb data from Tables I, II and III were used while the ^{119}Sn data were taken from the table presented by Ruby et al.[6] Thus, knowing the isomer shift for a compound of ^{121}Sb, one can predict the isomer shift of the analogous ^{119}Sn compound. There has been very much interest in obtaining the Mössbauer
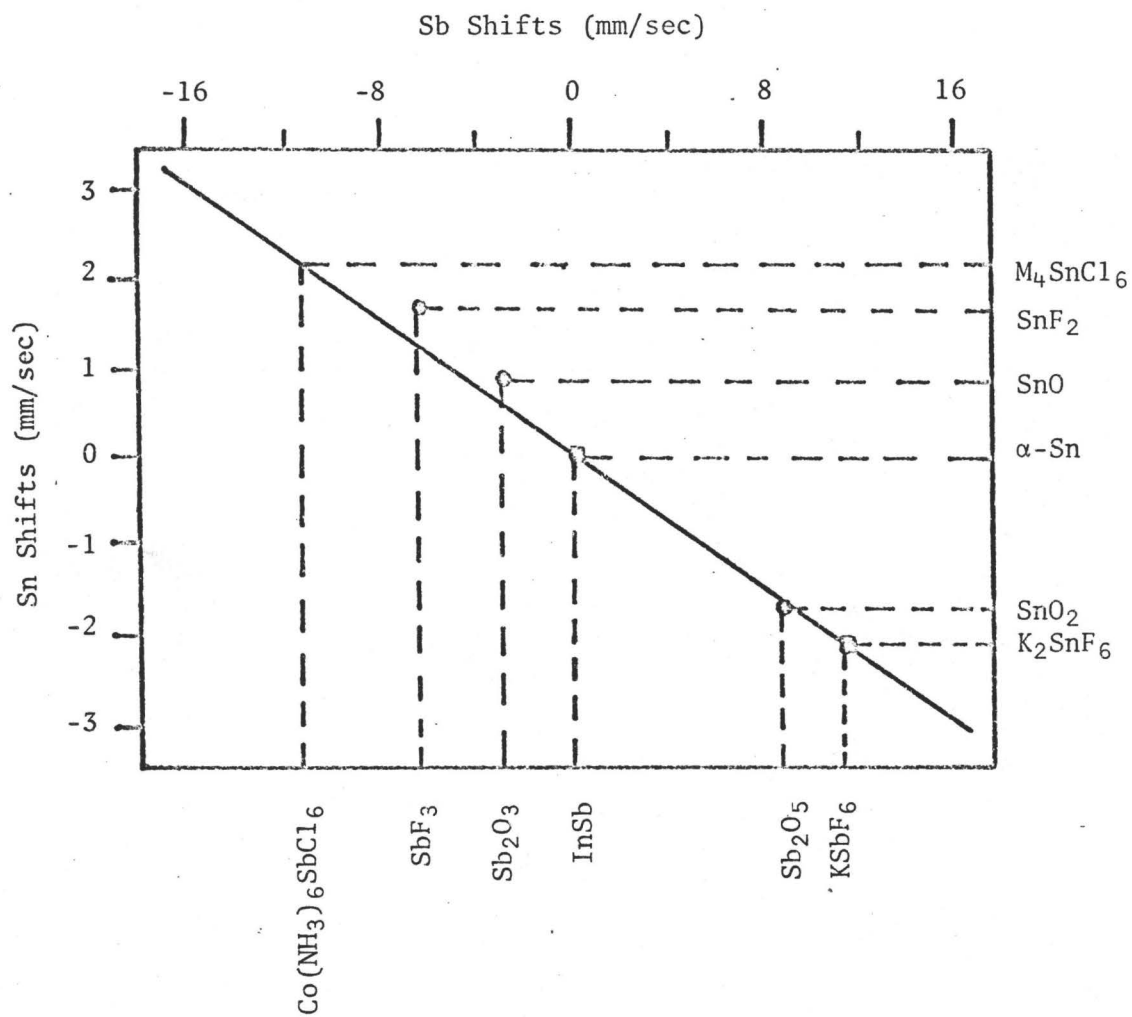
Figure 6. Comparison of ^{121}Sb and ^{119}Sn Isomer Shifts.

isomer shift of the bare Sn^{2+}.[54] Since the equivalent of a bare Sb^{3+} appears to have been reached in these hexachloroantimonate(III) salts, use of Ruby's correlation allows an estimate of the shift for an ionic Sn^{2+} to be made. Using the value (-11.2 mm/sec) for the most ionic hexachloroantimonate(III) salt, i.e., $Co(NH_3)_6SbCl_6$, a value of 2.2 mm/sec was obtained for the bare Sn^{2+} ion. This value is quoted relative to α tin or 2.2 + 2.1 = 4.3 mm/sec from $BaSnO_3$. This estimated shift for Sn^{2+} (4.3 mm/sec) might be realised in salts having the composition M_4SnCl_6. These salts, by analogy to the corresponding hexachloro Sb and Te salts, should have a stereochemically inactive lone pair. However, it may not be possible to stabilise six halogens about the Sn^{2+} because of the relatively low charge.

3. Antimony-Fluorine System I - Fluoro Anions of Antimony

The Mössbauer data are summarised in Table III and representative spectra are illustrated in Figure 7. Of the Sb(III) compounds examined the SbF_4^- and $Sb_2F_7^-$ ions have been reported as having novel structures: the $KSbF_4$ salt having a tetrameric anion $[Sb_4F_{16}]^{-4}$ with a square pyramidal arrangement about each antimony and a lone pair in the sixth coordination position;[38] $CsSb_2F_7$ contained discrete $Sb_2F_7^-$ ions with trigonal bipyramidal arrangement about each antimony with one of the equatorial positions being occupied by the lone pair.[36] These structures have been accepted and widely referred to for many years.[55] The structure of SbF_3 had been reported as consisting of discrete molecules with a pyramidal arrangement of fluorines about antimony.[56] Thus there appeared to be considerable variation in

TABLE III

Mössbauer Data for the Fluoro Anions of Antimony

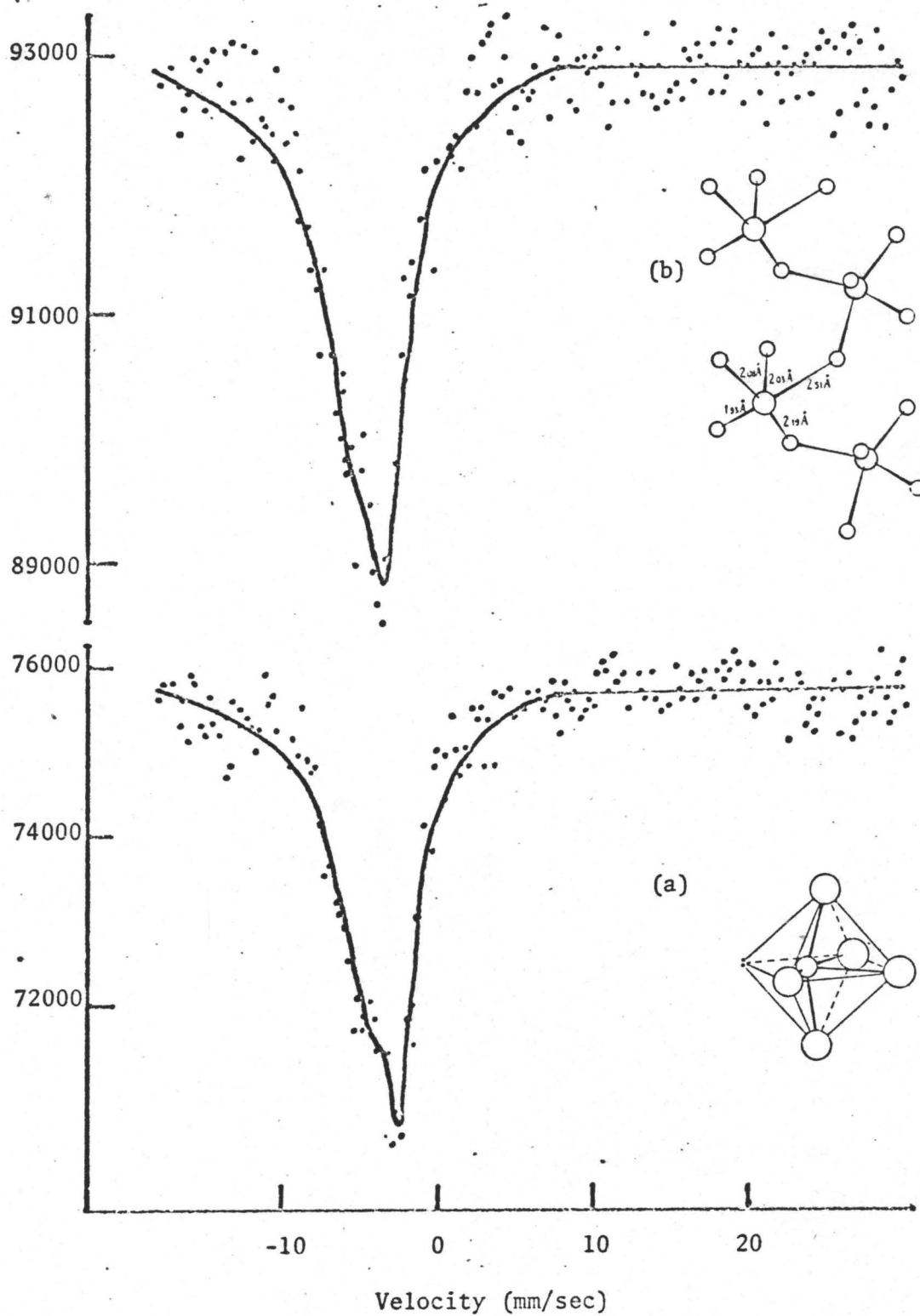| Compound	Isomer Shift (mm/sec)	Quadrupole Coupling Constant (e^2qQ) (mm/sec)
$(NH_4)_2SbCl_5$	-6.52 ± 0.11	$+11.2 \pm 1.8$
SbF_3 [6]	-6.04 ± 0.2	$+19.6 \pm 0.8$
$KSbF_4$	-5.02 ± 0.15	$+15.2 \pm 1.1$
$NaSbF_4$	-4.96 ± 0.09	$+15.1 \pm 1.0$
KSb_2F_7	-4.62 ± 0.09	$+17.0 \pm 0.9$
K_2SbF_5	-4.11 ± 0.09	$+16.1 \pm 0.6$
$KSbF_6$	$+11.42 \pm 0.03$	$+3.1 \pm 1.5$
$CsSb_2F_{11}$	$+10.95 \pm 0.06$	$+5.2 \pm 1.7$

Figure 7. Mössbauer Spectra: (a) K_2SbF_5, (b) $NaSbF_4$.

coordination about Sb(III) in these Sb-F systems and large variations in Mössbauer parameters might have been expected. In his later papers,[38,39] Bystrom revealed that he regarded the apparent changes in coordination number with some suspicion and suggested a reinvestigation of the structures of SbF_3, KSb_4F_{13} and $CsSb_2F_7$.

Recently Edwards[57] has shown that SbF_3 is not molecular, but polymeric with bridging fluorines to give an arrangement in which there are six fluorines about each antimony in a distorted octahedral arrangement, the distortion being the result of the stereochemically active 5s electron pair. The compound corresponding to the formula KSb_4F_{13} could not be prepared and probably does not exist. The data reported by Bystrom[35] for this stoichiometry could possibly have been due to a mixture of SbF_3 and KF.

Further evidence on the $Sb_2F_7^-$ anion has very recently[58] shown the previously accepted structure[36] to be incorrect. There are no discrete ions and this structure should be regarded as made up of SbF_4^- and SbF_3 units with interaction between units via fluorine bridges so that the whole structure resembles a chain. This results in two antimony environments, one six coordinate (5 fluorines and a lone pair) and the other five coordinate (4 fluorines and a lone pair). Mastin and Ryan[59] have also re-examined the data for $NaSbF_4$ and find this to be essentially as reported,[39] but they were unable to prepare suitable crystals of the corresponding potassium salt in order to check its structure. The sodium salt has each SbF_4^- ion sharing two fluorines with two other SbF_4^- units, so that each Sb has five fluorines and a lone pair to give a distorted octahedral arrangement about the antimony

(Figure 7b). The ion should be written as $[SbF_4]_n^{-n}$. A similarly distorted octahedral geometry is observed in the SbF_5^{-2} ion[37] (Figure 7a) as well as in the analogous chloro salt $(NH_4)_2SbCl_5$.[32]

Thus apart from SbF_3 and one site in KSb_2F_7 the environments about Sb(III) all appear to be distorted octahedral and the Mössbauer data in Table III are explained on this basis. The bonding can be described in terms of sp^3d^2 hybridization with an electron pair in one position of the octahedron. A comparison of the data for the $SbCl_5^{-2}$ and SbF_5^{-2} salts shows that the former has the higher "s" electron density at the Sb nucleus, the less electronegative chlorine being less efficient at removing electron density from the central antimony than is fluorine. There is still a more marked difference in quadrupole splitting between these two salts which can again be attributed to electronegativity differences in the halogens. Since the quadrupole splittings are all positive, the electric field gradient is negative and this implies an excess of electron density along the symmetry axis as compared to the equatorial plane. The four equatorial fluorines by virtue of their greater electron with-drawing power would therefore create more asymmetry than four chlorines and a greater quadrupole splitting results as is observed experimentally.

Since $NaSbF_4$ has been shown to have a chain structure, i.e., $(SbF_4)_n^{-n}$ by two independent groups,[39,59] it seems reasonable to suppose that the potassium salt with identical Mössbauer parameters will also have the same structure. The tetrameric structure proposed by Bystrom[38] for $KSbF_4$ may well be incorrect. The lower isomer shift and smaller quadrupole splitting compared to K_2SbF_5 indicate

that the bridging fluorines are less effective at removing electron density from the antimony than are terminal fluorines.

Examination of the KSb_2F_7 structure indicates two antimony sites, one with five near-neighbour fluorines and the other with four near fluorines. Both sites are very distorted due to the stereochemically active lone pair. It is impossible to resolve the Mössbauer spectrum for this compound into components due to each site, and the data reported are the result of fitting one eight-line pattern to the absorption envelope. The site having five fluorines might be expected to have an isomer shift close to that for SbF_5^{-2} while that having only 4 fluorines would be expected to have a higher "s" electron density and a lower shift. The "average" shift for KSb_2F_7 does turn out to be more negative than $KSbF_5$ and is consistent with the crystallographic data. The value for the quadrupole splitting for this compound cannot be interpreted in detail although the positive value is almost certainly correct. If $Sb_2F_7^-$ had had a structure where each antimony was surrounded by four fluorines and a lone pair of electrons in a distorted trigonal bipyramidal arrangement, then the lone pair in the equatorial plane would have produced a positive electric field gradient at the antimony and thus a negative value for the quadrupole splitting. This feature is not observed, adding support for the polymeric structure.[58]

The Mössbauer data for SbF_3 also fall into place as a result of the recent structure redetermination.[57] The polymeric nature of the SbF_3 results in six fluorines, all bridging, and a lone pair about each antimony. From this structure it seems likely that the Sb-F bonds

will have little "s" character, leaving the lone pair in an orbital with high "s" character. This results in high "s" electron density and a more negative isomer shift than for the other Sb(III) fluorides discussed above. Alternatively since all fluorines in this structure are bridging they will be less effective at removing charge from the nucleus and thereby leaving a relatively high "s" electron density at Sb. The large quadrupole splitting is clearly consistent with the distorted 7-coordinate structure.

Two salts of Sb(V) have been examined and the relevant data are given in Table III. Mössbauer data on SbF_6^- salts have been reported previously by Ruby et al.[6] and Brukhanov et al.[8] The isomer shift of the sodium salt is 10.4 ± 0.2 mm/sec[8] while that for the potassium salt is given as 12.3 ± 0.4 mm/sec,[6] both with respect to InSb. The isomer shift for $KSbF_6$ obtained in this laboratory was 11.42 ± 0.03 mm/sec, but a direct comparison between our data and that of Ruby et al.[6] may not be valid since they recorded their spectrum at 4.2°K. However since our data and that of the Russian workers[8] both refer to InSb at liquid nitrogen temperature a comparison is allowable. The sodium salt has a lower isomer shift than the potassium salt by 1 mm/sec. Part of this difference may be experimental error but it is interesting to note that these salts do have different crystal structures. Sodium hexafluoroantimonate(V)[60] has the same structure as $LiSbF_6$,[61] with a perfect octahedron of fluorines about each antimony. However in the $KSbF_6$ this octahedron is distorted.[62] It is also noted that the Sb-F bond length is 1.877 Å in $LiSbF_6$ but 1.77 Å in $KSbF_6$. Such differences are significant and if the sodium salt has the same

Sb-F bond length as that found in LiSbF$_6$ then the difference in isomer shift between NaSbF$_6$ and KSbF$_6$ is understandable.

The fluorines in the Na salt probably have more bridging character than fluorines in the K salt. These bridging fluorines are less effective at withdrawing electrons leading to a higher "s" electron density at the nucleus and a more negative shift for the Na salt. However only the data for LiSbF$_6$ can be considered accurate and the others should probably be reinvestigated.

Brukhanov et al.[8] found no quadrupole splitting in the sodium hexafluoroantimonate(V) as would have been expected for the regular octahedral arrangement discussed above. A splitting was reported for the KSbF$_6$,[6] which we confirm, although our value is considerably less (+3.1 mm/sec) than that previously reported (+8.0 mm/sec).[6] Both results confirm that this salt indeed has a distorted anion. We feel that our lower value is the more realistic view of the crystallographic evidence.

The data for the Sb$_2$F$_{11}^-$ salt can be rationalised on terms of the known structural information. Although the structure of the Cs salt is unknown it seems reasonable that the anion will resemble that in XeF·Sb$_2$F$_{11}$,[63] where there are two SbF$_5$ units linked by a fluorine bridge. Since a bridging fluorine will remove less electron density from the central atom than a terminal fluorine, one would expect the Sb in Sb$_2$F$_{11}^-$ to have a higher "s" electron density than in SbF$_6^-$, and hence a lower isomer shift and this is observed experimentally. Moreover, there is a larger quadrupole splitting in Sb$_2$F$_{11}^-$ than in SbF$_6^-$. In the Sb$_2$F$_{11}^-$ fragment of XeF·Sb$_2$F$_{11}$, there are three Sb-F

distances 1.78 - 1.80 Å and 1.90 - 1.93 Å for the two kinds of terminal fluorine, and a longer bond 2.05 Å to the bridging fluorine. The quadrupole splitting found for $CsSb_2F_{11}$ is clearly in accord with a distorted antimony environment.

4. Antimony-Fluorine System II - Complex Fluorides and Fluorosulphates

The reactions of antimony trifluoride with the pentafluorides of arsenic and antimony in sulfur dioxide yielded the 1:1 adducts $SbF_3 \cdot SbF_5I$, $SbF_3 \cdot AsF_5$, $SbF_3 \cdot SbF_5II$, and $SbF_3 \cdot SbF_5III$. The pentafluorides are strong Lewis acids. Interaction between the MF_5 and SbF_3 could result in the abstraction of a fluoride ion from SbF_3 to give, in the completely ionic situation, $SbF_2^+MF_6^-$. T. Birchall et al.[64] have reported the Raman spectra of the adducts $SbF_3 \cdot SbF_5I$ and $SbF_3 \cdot AsF_5$. The data indicates that the MF_6^- anion has lower than the expected O_h symmetry. They postulate that this lowering of symmetry occurs as a result of fluorine bridging to the cation. These strong cation-anion interactions in the SbF_3 adducts present a situation not unexpected in view of the high Lewis acidity of the SbF_2^+ cation. It was hoped that Mössbauer spectroscopy would provide information as to the character of these adducts.

Details of the [121]Sb Mössbauer spectra are presented in Table IV. The spectra of the adducts $SbF_3 \cdot AsF_5$ and $SbF_3 \cdot SbF_5I$ are illustrated in Figure 8. The spectrum of $SbF_3 \cdot SbF_5I$ adduct shows two resonance absorptions of equal area, and this together with the analytical and Raman data confirm a 1:1 adduct.[64] The higher velocity absorption is due to a Sb(V) species with six near fluorine neighbours, the shift being in the range of SbF_6^- and $Sb_2F_{11}^-$ salts. The possibility of the

TABLE IV

Mössbauer Data for the Complex Antimony Fluorides and Fluorosulphates

	Compound	Isomer Shift (mm/sec)	Quadrupole Coupling Constant (e^2qQ) (mm/sec)
1.	$SbF_3 \cdot SbF_5 I$	$- 8.27 \pm 0.18$ $+11.29 \pm 0.05$	$+18.2 \pm 2.9$ $+ 8.0 \pm 2.0$
2.	$SbF_3 \cdot AsF_5$	$- 7.28 \pm 0.12$	$+19.4 \pm 1.3$
3.	$SbF_3 \cdot SbF_5 II$[*]	$- 7.25 \pm 0.16$ $+10.98 \pm 0.08$	
4.	$SbF_3 \cdot SbF_5 III$	$- 8.18 \pm 0.12$ $+11.32 \pm 0.07$	$+18.1 \pm 1.5$ $+ 2.0 \pm 7.0$
5.	$Sb(SO_3F)_3$ or $SbF_3 \cdot 3SO_3$	$- 8.88 \pm 0.10$	$+ 4.4 \pm 9.5$
6.	$SbAsF_6$	$- 6.04 \pm 0.13$	$+16.2 \pm 2.0$
7.	$SbSb_2F_{11}$[*]	$- 7.20 \pm 0.3$ $+11.15 \pm 0.02$	
8.	$SbSO_3F$	$- 7.60 \pm 0.09$	$+19.4 \pm 1.0$
9.	$Sb_8(Sb_2F_{11})_2$[*]	$- 7.25 \pm 0.20$ $- 3.13 \pm 0.10$ $+11.16 \pm 0.05$	
10.	Sb metal[*]	$- 3.02 \pm 0.1$	
11.	SbF_3[6]	$- 6.04 \pm 0.2$	$+19.6 \pm 0.8$

[*] Computer fitted to Lorenztian line shape.
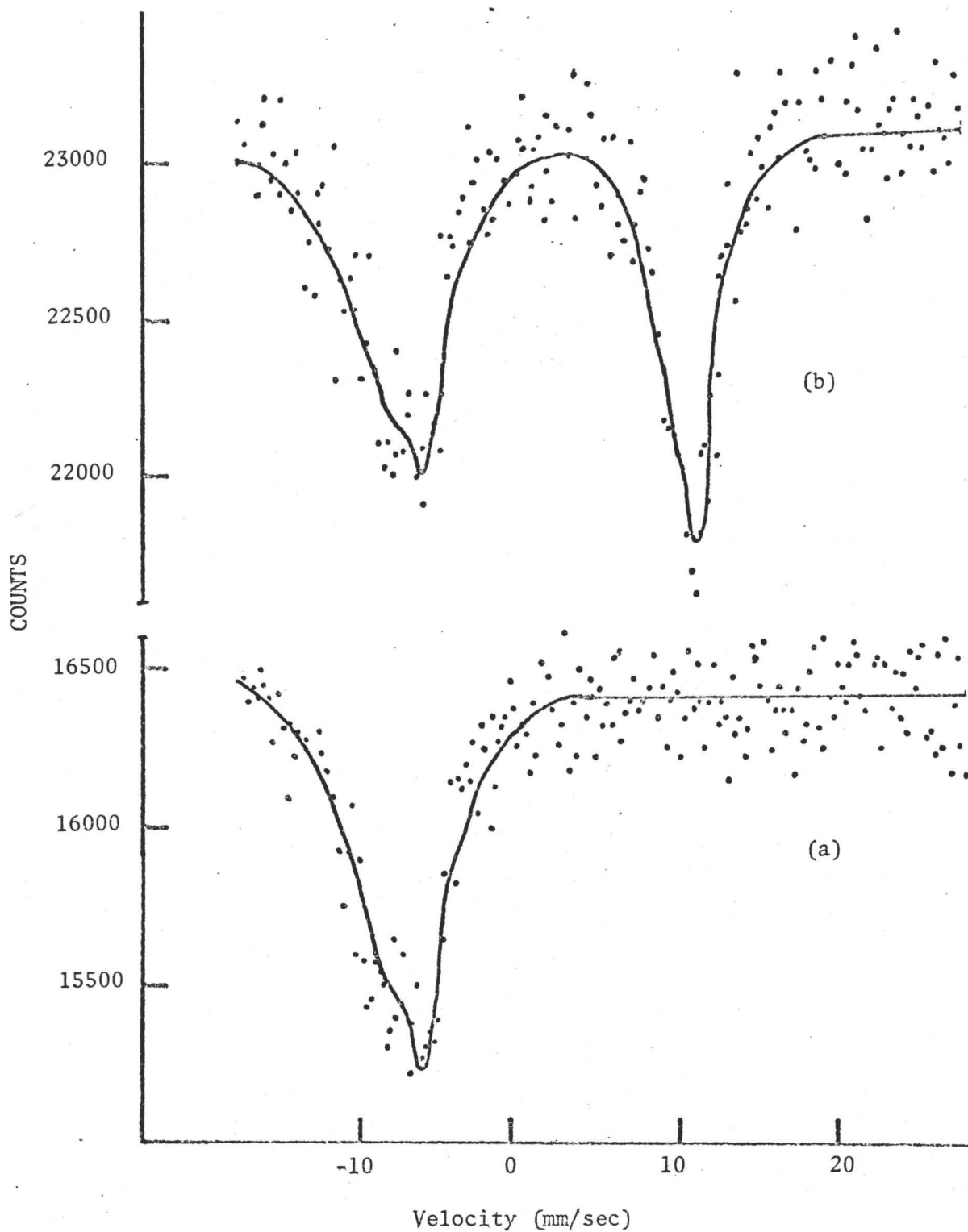
Figure 8. Mössbauer Spectra: (a) $SbF_3 \cdot AsF_5$, (b) $SbF_3 \cdot SbF_5I$.

anion being $Sb_2F_{11}^-$ is eliminated by the analytical, Raman and ^{19}F NMR data.[64] Antimony(V) in a fluorine environment having O_h symmetry would have zero quadrupole splitting. The significant splitting observed in this complex indicates that the environment is distortéd, confirming the Raman spectral data.[64]

In the Sb(III) region of the spectrum the broad asymmetric absorption occurs at lower velocity than SbF_3 indicating a higher "s" electron density at the antimony nucleus with the $SbF_3 \cdot SbF_5I$ having a lower isomer shift than $SbF_3 \cdot AsF_5$. Within experimental error, the quadrupole coupling constant for the two adducts are very similar to that in SbF_3. The structure of SbF_3 was shown to be polymeric with a seven coordinate arrangement of six fluorines and a lone pair.[57] Adduct formation with either AsF_5 or SbF_5 does not appear to result in drastic changes in symmetry about the Sb(III) site since the quadrupole splitting is not significantly altered. The three long Sb-F bonds in SbF_3 could have been replaced, in the adducts, by long bridge bonds to the fluorines of the anion. The changes observed in isomer shift can be explained by the involvement of one of the SbF_3 fluorines in a bridged bond to the MF_5. Since these bonds probably have little "s" character, as evidenced by the small F-Sb-F angle (87.3°), a lengthening of this bond would remove p or d electrons from the vicinity of the Sb(III) thus decreasing the shielding of the "s" electrons from the nucleus. This results in an increase in "s" electron density and hence a lowering of the isomer shift. In the extreme case, the adducts formed would be completely ionic as $SbF_2^+MF_6^-$. The evidence presented above is con-

sistent with an intermediate situation where there is considerable bridging between anion and cation. Since SbF_5 is a stronger Lewis acid than AsF_5, the $SbF_3 \cdot SbF_5 I$ adduct approaches the ionic situation more closely and thus has a lower isomer shift. The adduct $SbF_3 \cdot SbF_5 III$ has almost identical isomer shift and quadrupole coupling parameters to that of $SbF_3 \cdot SbF_5 I$. Presumably forms I and III are identical though $SbF_3 \cdot SbF_5 III$ is crystalline whereas $SbF_3 \cdot SbF_5 I$ is not. The other adduct $SbF_3 \cdot SbF_5 II$ has an isomer shift in the Sb(III) region comparable to that for the $SbF_3 \cdot AsF_5$ adduct. It is likely then that the cation-anion interaction is similar to that for the $SbF_3 \cdot AsF_5$ adduct, i.e., it is a less ionic compound than its isomer $SbF_3 \cdot SbF_5 I$.

The compound, first formulated $Sb(SO_3F)_3$, shows the most negative isomer shift of the Sb(III) compounds in this group indicating a greater "s" electron density at the nucleus. The spectrum obtained for this compound was not very well resolved with the result that there is a large error in the quadrupole coupling constant though the isomer shift parameter is quite accurate.

The fluorosulphate ligands could be associated with the antimony through either the oxygen or fluorine atoms. The range of isomer shifts for antimony(III) bonded to oxygen is -6.0 mm/sec to -3.0 mm/sec The isomer shift for this compound (-8.88 mm/sec) is very much below the lower limit of -6.0 mm/sec, strongly suggesting that the Sb is not coordinated by oxygens but rather by fluorines. As yet there has been no structural information regarding the bonding of antimony with fluorosulphate ligands. Evidence for the above formulation,

$Sb(SO_3F)_3$ has not been forthcoming and another possible formulation could be $SbF_3 \cdot 3SO_3$. This adduct could be considered to be similar in nature to the above-mentioned $SbF_3 \cdot MF_5$ adducts. In this case each SO_3 could accept a fluorine to form a bridge bond between Sb and S. The antimony, as a result, could approach Sb^{3+} which of course would have a very low isomer shift.

Unusual oxidation states are known to exist in polyatomic cations of such elements as Bi, Te, Se, S, and Sb.[65] Since the Mössbauer technique is useful for detecting different oxidation states, compounds 6-8, which have a formal oxidation state of one were examined in an attempt to confirm this oxidation state. A purely ionic Sb^{1+} would have an electron configuration $5s^2 5p^2$. The loss of one p electron would decrease the shielding of the s electrons at the Sb nucleus causing the "s" electron density to increase thus lowering the isomer shift compared to zero valent Sb metal. Theoretically the isomer shift for a Sb(I) compound should be more negative than Sb(O) and less negative than a Sb(III) compound of comparable structure. However the Sb(III) range of isomer shifts is considerable and overlaps those of the Sb(I) compounds thus precluding any unambiguous assignment of a shift defining a Sb(I) oxidation state. The large negative isomer shifts imply a fairly large "s" electron density at the antimony nucleus. Thus the structure and hybridization scheme for bonding would have to be taken into account in order to assign the Mössbauer parameters correctly. If these compounds, formally classified as Sb(I), are clusters with Sb-Sb bonds, i.e., $[Sb_n]^{n+}$ then the cation would behave as if it were in a higher oxidation state, e.g., (III) and its Mössbauer

parameters would resemble those of Sb(III). This was found to be the case for organic compounds of formally divalent tin, e.g., R_2Sn.[66,67] They had isomer shifts in the Sn(IV) region of the spectrum and were considered to be polymeric species containing both Sn-Sn and Sn-C bonds. A similar situation could exist for these Sb(I) systems again with extensive F bridging between cation and anion to account for the low isomer shifts. The large quadrupole coupling constants for $SbAsF_6$ (Figure 9b) and $SbSO_3F$ suggest a very distorted arrangement about the antimony which is in accord with any of the above possible antimony-ligand arrangements.

The compound $Sb_8(Sb_2F_{11})_2$ was thought to contain the polyatomic cation Sb_8^{2+} in which the antimony would have an oxidation state of 1/4. This material was a greyish colour and there was the possibility that this was, in fact, a mixture of black antimony metal and a white Sb(III) or Sb(I) compound. The spectrum showed two absorptions, one at +11.66 mm/sec typical of Sb(V), which has been shown to be due to the $Sb_2F_{11}^-$ anion by ^{19}F NMR. The other peak occurred at $\sim$-3.6 mm/sec. The broad asymmetric resonance at the lower velocity could be due either to a very distorted antimony environment or possibly more than one antimony site. The asymmetric portion of this peak was unusual in that it occurred more towards the baseline of the spectrum (Figure 9a) rather than near the resonance maximum, further suggesting a mixture. The spectrum was fitted to both three and two line patterns with the three line pattern giving the better fit (Figure 9a). Thus the large peak (-3.13 mm/sec) is attributed to Sb metal with the wing peak (-7.25 mm/sec) assigned to either a Sb(III) or Sb(I) compound. Thus, the
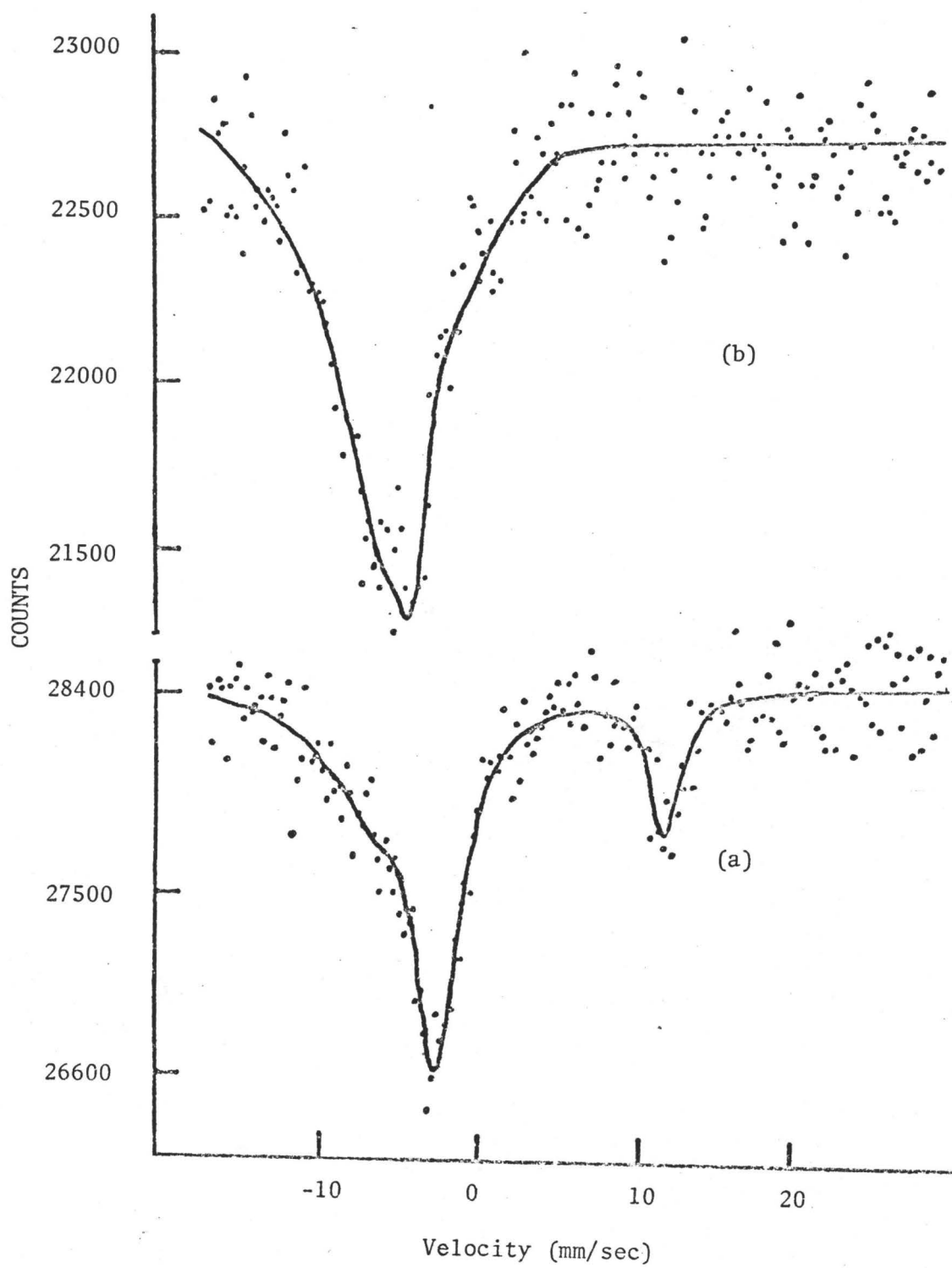
Figure 9. Mössbauer Spectra: (a) $Sb_8(Sb_2F_{11})_2$, (b) $SbAsF_6$.

Sb_8^{2+} cation is probably not present in this compound.

The above discussion is somewhat limited in scope due to the lack of other physiochemical information on the above compounds (1-9). As more information becomes available the Mössbauer parameters can be interpreted in a more definite sense.

5. Antimony Minerals

The data for the three minerals Nadorite ($PbSbO_2Cl$), Tetrahedrite ($Cu_{12}Sb_4S_{13}$), and Boulangerite ($Pb_5Sb_4S_{11}$) are summarised in Table V. Sillén and Melander[68] reported the structure of nadorite as being made up of [$PbSbO_2$] layers with Cl^- ions located between them. These layers consist of alternate square pyramidal SbO_4 and PbO_4 groups, the Sb-O distance being 2.17 Å. The nearest chlorines (four of them) to each antimony are at a distance of 3.39 Å on the opposite side of the Sb compared to the oxygens. This distance is greater than the sum of the covalent radii (2.40 Å) but is less than the sum of the Van der Waal's radii (4.26 Å). This suggests that there is some inter-action between the antimony and the four chlorines though this is probably quite weak. The next nearest Cl atoms are at a distance of approximately 5.0 Å. Such large distances rule out any interaction between these chlorines and the antimony. If one disregards all chlorines, then the antimony is situated at the apex of an undistorted square pyramid of oxygen atoms. This type of oxygen coordination is similar to that in $SbPO_4$ and to the Sb(III) site in Sb_2O_4, where there is also a one-sided coordination to four oxygen atoms. However, the isomer shift for nadorite (-3.22 mm/sec) is much more positive than those for $SbPO_4$ and Sb_2O_4 indicating a lower "s" electron density

TABLE V

Mössbauer Data for the Antimony Minerals

Compound	Isomer Shift (mm/sec)	Quadrupole Coupling Constant (mm/sec)	% A
Nadorite ($PbSbO_2Cl$)	-3.22 ± 0.1	+15.0 ± 1.0	14.0
Tetrahedrite ($Cu_{12}Sb_4S_{13}$)	-5.91 ± 0.04	+11.0 ± 0.7	12.0
Boulangarite ($Pb_5Sb_4S_{11}$)	-4.10 ± 0.1	+14.4 ± 1.0	8.6

at the antimony nucleus. This difference could be due to influence of the four chlorines at 3.39 Å which could withdraw "s" electron density from the vicinity of the Sb nucleus causing an increase in isomer shift. The quadrupole coupling constant (+15.0 ± 1.0 mm/sec) is consistent with a distorted environment about the antimony (Figure 10a). However, this quadrupole coupling constant is slightly smaller than those found in Sb_2O_4 (+16.4 ± 0.6) and $SbPO_4$ (+18.4 ± 0.7). Possibly the four chlorines above the Sb plane help to reduce the asymmetry about the Sb nucleus as compared to the above two compounds which have a strictly one-sided coordination of oxygen atoms.

In antimony sulphide systems the most common type of coordination consists of a trigonal-pyramidal arrangement of sulphurs with three unlike bonds varying in length from 2.4 Å to 2.7 Å (sum of covalent radii Sb-S = 2.42 Å).[47] This basic polyhedron can be made into a square pyramid by two elongated bonds (2.8 to 3.1 Å) or into a distorted octahedron by contacts at distances from 3.1 Å to 3.8 Å which are within the limits of the sum of the Van der Waal's radii (4.29 Å). In the case of the pentacoordinate square pyramidal configuration, the Sb atoms are below the basal plane of the pyramid and away from the apex presumably as a result of lone pair-bond pair interactions.[69] Sb_2S_3 with its two different antimony sites exemplifies the main features of coordination in the antimony sulphide system. One Sb site has a trigonal pyramidal coordination with Sb-S distances 2.57(2) and 2.58 Å (1). This coordination becomes a distorted octahedral when contacts with the three sulphur atoms at 3.15 (2) and 3.20 Å (1) are considered. The second Sb site is surrounded by five sulphur atoms at
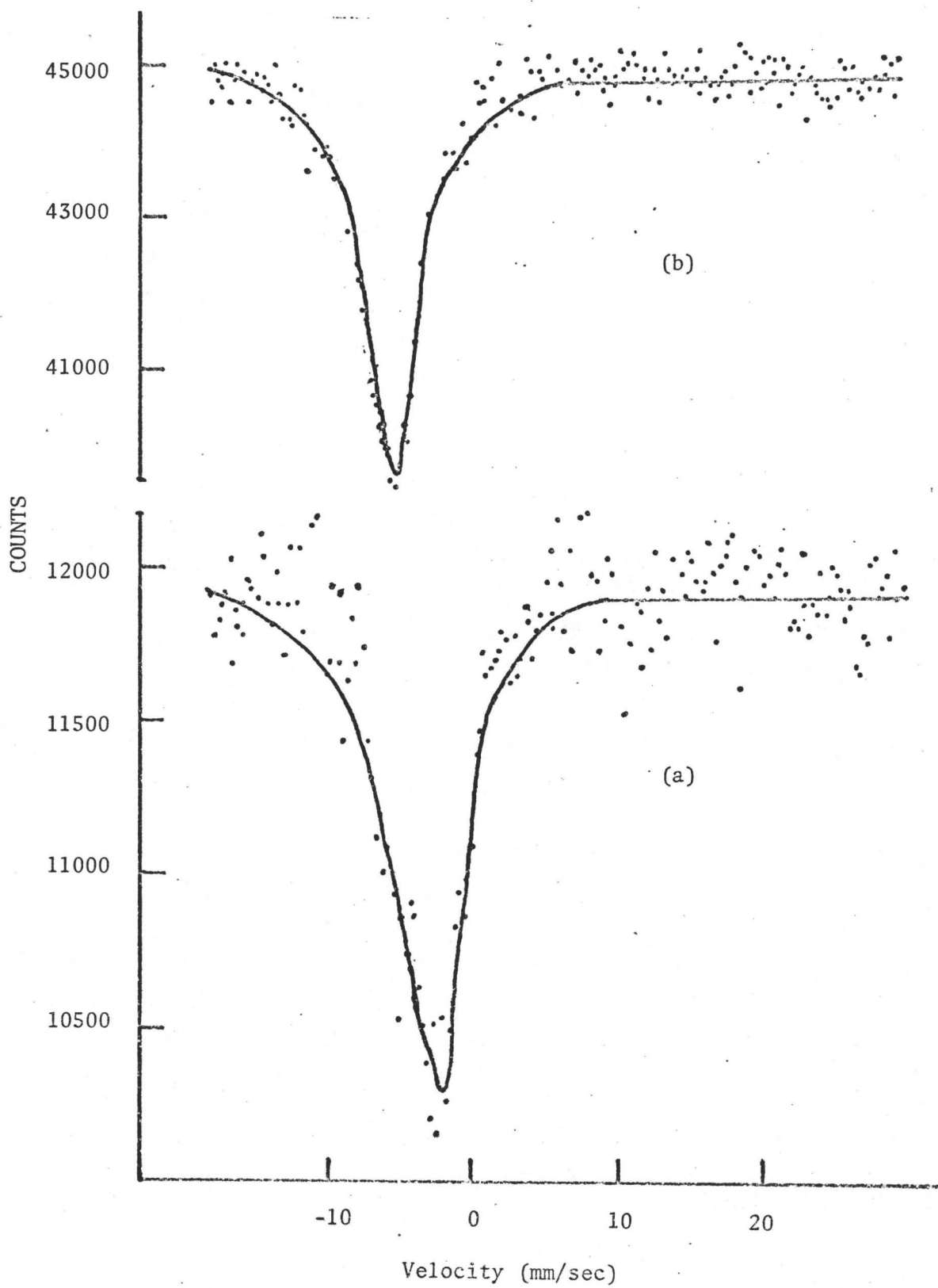
Figure 10. Mössbauer Spectra: (a) Nadorite, (b) Tetrahedrite.

distances 2.49(1), 2.68(2) and 2.83 Å (2) forming a square pyramid with the Sb atom displaced from the basal plane as mentioned above.[47]

The structure of tetrahedrite consists of a trigonal pyramidal arrangement of sulphur atoms about the antimony with the three Sb-S bond distances being of equal length (2.436 Å).[70] Thus this sulphide system is an exception to the above general rule, i.e., that the Sb-S distances are different. Also the Sb-S bond distances are considered short for the antimony-sulphide system as the lower limit in bond length is 2.4 Å. These short bond distances along with the ortho-gonal direction of the bonds suggests a strong bond involving p^3 hybrids. The isomer shift of tetrahedrite (-5.91 mm/sec) is similar to that for Sb_2S_3 (-6.0 mm/sec) which contains two antimony sites, the isomer shift being an average of the two sites. It is interesting to note that all of the Sb-S bond lengths in either site of Sb_2S_3 are longer than the Sb-S lengths in tetrahedrite. The electron with-drawing effect of the three close sulphurs in tetrahedrite is similar to the average effect of the more distant sulphurs in both sites of Sb_2S_3. The quadrupole coupling constant (+11.0 ± 0.7 mm/sec) in tetrahedrite suggests an unsymmetrical environment about the Sb as one would expect in this distorted tetrahedral structure including the lone pair (Figure 10b). Since no other quadrupole splitting data has been reported on such sulphide systems one cannot comment accurately upon the magnitude of the splitting as to its size compared to the norm. It would seem reasonable that the three equal bond lengths would lessen the asymmetry about the antimony as compared to the usual three unequal Sb-S lengths. Thus other antimony-sulphides having

unequal bond lengths would probably have larger quadrupole splittings.

The structure of boulangerite is unknown.[71] The more positive isomer shift compared to tetrahedrite and Sb_2S_3 indicates a lower "s" electron density at the antimony nucleus. This fact would probably rule out the tetrahedrite type structure of short, equal Sb-S bond lengths. It could have a trigonal pyramidal arrangement of sulphurs if the Sb-S bonds contained more s character than the bonds in tetrahedrite thus reducing the "s" electron density at the nucleus. Another possibility is a pentacoordinate antimony forming a square pyramidal configuration. The five sulphurs could withdraw more "s" electron density from the Sb nucleus than the three short orthogonal bonds in tetrahedrite thus increasing the shift. Also the larger quadrupole coupling constant ($+14.4 \pm 1.0$ mm/sec) indicates a greater asymmetry about the antimony. Unequal bond lengths would make for a more asymmetric environment and result in a larger quadrupole splitting.

REFERENCES

1. Y. Y. Chu, O. C. Kistner, A. C. Li, S. Monaro, and M. L. Perlman, Phys. Rev., 133, 1361 (1964).

2. R. L. Auble, W. H. Kelley, and H. H. Bolotin, Nucl. Phys., 58, 337 (1964).

3. R. E. Snyder and G. B. Beard, Phys. Letters, 15, 264 (1965).

4. S. L. Ruby, G. M. Kalvius, G. B. Beard, and R. E. Snyder, Phys. Rev., 148, 176 (1966).

5. S. L. Ruby and G. M. Kalvius, Phys. Rev., 155, 353 (1967).

6. S. L. Ruby, G. M. Kalvius, G. B. Beard, and R. E. Snyder, Phys. Rev., 159, 239 (1967).

7. S. L. Ruby, Mössbauer Effect Methodology, Plenum Press, New York, Vol. 3, 1969.

8. V. A. Brukhanov, B. Z. Iofa, V.Kotkhekar, S. I. Semenov, and V. S. Shpinel, Soviet Phys. J.E.T.P., 26, 912 (1968).

9. V.Kotkhekar, B. Z. Iofa, S. I. Semenov, and V. S. Shpinel, Soviet Phys. J.E.T.P., 28, 86 (1969).

10. S. E. Gukasyan and V. S. Shpinel, Phys. Status Solidi, 29, 49 (1968).

11. G. G. Long, J. G. Stevens, L. H. Bowen, and S. L. Ruby, Inorg. Nucl. Chem. Letters, 5, 21 (1969).

12. G. G. Long, J. G. Stevens, and L. H. Bowen, Inorg. Nucl. Chem. Letters, 5, 799 (1969).

13. L. H. Bowen, J. G. Stevens, and G. G. Long, J. Chem. Phys., 51, 2010 (1969).

14. G. G. Long, J. G. Stevens, R. J. Tullbane, and L. H. Bowen, J. Amer. Chem. Soc., 92, 4230 (1970).

15. J. G. Stevens and S. L. Ruby, Phys. Letters, 32A, 91 (1970).

16. G. G. Long and L. H. Bowen, Inorg. Nucl. Chem. Letters, 6, 837 (1970).

17. H. Z. Dokuzoguz, L. H. Bowen, and H. H. Stadelmaier, Solid State Comm., 8, 259 (1970).

18. V. A. Golovnin, S. M. Irkaev, R. N. Kuz'min, and V. V. Mill, J.E.T.P. Letters, 11, 21 (1970).

19. R. L. Mössbauer, A. Physik, 151, 124 (1958).

20. R. L. Mössbauer, Naturwiss., 45, 538 (1958); Z. Naturforsch., 149, 211 (1959).

21. A. J. F. Boyle and H. E. Hall, Reports Progr. Phys., 25, 441 (1962).

22. H. Frauenfelder, The Mössbauer Effect, New York, W. A. Benjamin, Inc., 1962.

23. R. H. Herber and H. H. Stockler, Trans. New York Acad. Sci., 26, 929 (1964).

24. J. G. Stevens and L. H. Bowen, Mössbauer Effect Methodology, Plenum Press, New York, Vol. 5, 1969.

25. V. I. Goldanskii, E. F. Makarov, and V. V. Khrapov, Phys. Letters, 3, 344 (1963).

26. V. I. Goldanskii, E. F. Makarov, and V. V. Khrapov, Soviet Phys. J.E.T.P., 17, 508 (1963).

27. S. V. Karyagin, Doklady Akad. Nauk. S.S.S.R., 148, 1102 (1963).

28. G. Brauer, Handbook of Preparative Inorganic Chemistry, Vol. 1, Academic Press, New York, 1963.

29. A. I. Vogel, A Textbook of Quantitative Inorganic Analysis, Theory and Practise, 2nd Ed., Longmans, Green, London, New York, 1951.

30. P. Pascal, Nouveau Traité de Chimie Minérale, Masson et Cie, Paris, Vol. XI, 1958.

31. E. Martineau and J. B. Milne, J. Chem. Soc. (A), 2971 (1970).

32. E. Edstrand, M. Inge, and N. Ingri, Acta Chem. Scand., 9, 122 (1955).

33. R. F. Weinland and H. Schmid, Chem. Ber., 38, 1083 (1905).

34. T. Barrowcliffe, I. R. Beattie, P. Day, and K. Livingston, J. Chem. Soc. (A), 1810 (1967).

35. A. Bystrom and K. A. Wilhelmi, Arkiv Kemi, 3, 17 (1951).

36. A. Bystrom and K. A. Wilhelmi, Arkiv Kemi, 3, 373 (1951).

37. A. Bystrom and K. A. Wilhelmi, Arkiv Kemi, $\underline{3}$, 461 (1951).

38. A. Bystrom, S. Bückland, and K. A. Wilhelmi, Arkiv Kemi, $\underline{4}$, 175 (1952).

39. A. Bystrom, S. Bückland, and K. A. Wilhelmi, Arkiv Kemi, $\underline{6}$, 77 (1953).

40. A. F. Wells, Structural Inorganic Chemistry, Oxford University Press, 1962.

41. H. Krebs, Inorganic Crystal Chemistry, McGraw-Hill, London, 1968.

42. F. M. Jaeger and H. S. van Klooster, Z. anorg. Chem., $\underline{78}$, 245 (1912).

43. A. Grund and A. Preisinger, Acta Cryst., $\underline{3}$, 363 (1950).

44. A. C. Skapski and D. Rogers, Proc. Chem. Soc., $\underline{1}$, 400 (1970).

45. A. C. Skapski and D. Rogers, Chem. Comm., 611 (1965).

46. B. Kinberger, Acta Chem. Scand., $\underline{24}$, 320 (1970).

47. T. N. Polynova and M. A. Porai-Koshits, J. Struct. Chem. (USSR), $\underline{7}$, 147 (1966).

48. S. L. Lawton and R. A. Jacobson, Inorg. Chem., $\underline{5}$, 743 (1966).

49. M. B. Robin and P. Day, Adv. Inorg. Chem. Radiochem., $\underline{10}$, 247 (1967).

50. G. G. Long, R. J. Tullbane, and L. H. Bowen, Abstracts 158th Amer. Chem. Soc. Meeting, New York, September 1969.

51. K. A. Jensen, Z. anorg. allg. Chem., $\underline{232}$, 193 (1937).

52. P. Day, J. Chem. Soc. (A), 2423 (1969).

53. C. J. Adams and A. J. Downs, Chem. Comm., 1699 (1970).

54. T. Birchall, P. A. W. Dean, and R. J. Gillespie, J. Chem. Soc. (A), 1971 (in press).

55. F. A. Cotton and G. Wilkinson, Advanced Inorganic Chemistry, 2nd Ed., Interscience, New York, 1967.

56. A. Bystrom and A. Westgren, Arkiv Kemi Miner., $\underline{17}$, 1 (1943).

57. A. J. Edwards, J. Chem. Soc. (A), 2751 (1970).

58. S. H. Mastin and R. R. Ryan, Inorg. Chem. 1971 (in press).

59. S. H. Mastin and R. R. Ryan, (private communication).

60. H. Bode and H. Clausen, Z. anorg. Chem., 265, 229 (1951).

61. J. H. Burns, Acta Cryst., 15, 1098 (1962).

62. H. Bode and E. Voss, Z. anorg. Chem., 264, 144 (1951).

63. V. M. McRae, R. D. Peacock, and D. R. Russel, Chem. Comm., 62 (1969).

64. T. Birchall, P. A. W. Dean, B. DellaValle, and R. J. Gillespie, Submitted to Can. J. Chem.

65. R. J. Gillespie and J. Passmore, Submitted to Accounts of Chem. Research.

66. G. K. Ingham, S. D. Rosenberg, and H. Gilman, Chem. Rev. 60, 459 (1960).

67. V. I. Goldanskii, V. Y. Rochev, and V. V. Khrapov, Proc. Acad. Sci. USSR Phys. Chem. Sect., 156, 571 (1964).

68. L. G. Sillén and L. Melander, Z. Krist., 103, 420 (1941).

69. D. Grdenic and S. Scavnicar, Proc. Chem. Soc., 147 (1960).

70. B. J. Wuensch, Science, 141, 804 (1963).

71. E. Hellner, Jour. Geol., 66, 503 (1958).